

Kinetics of Ring Inversion in Strongly Nonplanar Iron(III) Octaalkyltetraphenylporphyrinates

Liliya A. Yatsunyk, Hiroshi Ogura, and F. Ann Walker*

Department of Chemistry, University of Arizona, Tucson, Arizona 85721-0041

Received July 9, 2004

The dynamics of porphyrin ring inversion of a number of Fe(III) complexes of octamethyltetraphenylporphyrin, (OMTPP)Fe^{III}; octaethyltetraphenylporphyrin, (OETPP)Fe^{III}; octaethyltetra(perfluorophenyl)porphyrin, (F₂₀OETPP)-Fe^{III}; and tetra- β,β' -tetramethylenetetraphenylporphyrin, (TC₆TPP)Fe^{III}, having either one (Cl⁻, ClO₄⁻) or two [4-(dimethylamino)pyridine, 4-Me₂NPY; 1-methylimidazole, 1-Melm; *tert*-butylisocyanide, *t*-BuNC; or cyanide, CN⁻] axial ligands have been characterized by 1D dynamic NMR (DNMR) and 2D ¹H NOESY/EXSY spectroscopies as a function of temperature. The activation parameters, ΔH^\ddagger , ΔS^\ddagger , and ΔG^\ddagger_{298} , and the extrapolated rate constants at 298 K for three chloride, one perchlorate, and three bis-(4-Me₂NPY) complexes as well as [FeOETPP(1-Melm)₂]-Cl, [FeOETPP(*t*-BuNC)₂]ClO₄, and Na[FeOETPP(CN)₂] have been determined. The results indicate that there is a wide range of flexibility for the porphyrin core ($k_{\text{ex}}^{298} = 10\text{--}10^7 \text{ s}^{-1}$) that decreases in the order TC₆TPP > OMTPP > F₂₀OETPP \geq OETPP, which correlates with increasing porphyrin nonplanarity. To determine the effect of axial ligands, we calculated the free energy of activation, ΔG^\ddagger_{298} for OETPPFe^{III} bis-ligated with 4-Me₂NPY, 1-Melm, or 4-CNPy ($\sim 59 \text{ kJ mol}^{-1}$), and for complexes with small cylindrical ligands (*t*-BuNC and CN⁻) ($\sim 37 \text{ kJ mol}^{-1}$). These data suggest that the ΔG^\ddagger_{298} for planar ligand rotation is roughly 20–25 kJ mol⁻¹.

Introduction

Iron(III) synthetic porphyrin complexes have been utilized widely as potential models of heme centers in proteins.¹ Yet, whereas the rotation and exact orientation of the axial ligands in heme proteins are tightly controlled by covalent attachment of the axial ligands (histidine imidazole, methionine thioether, etc.) to the protein backbone, hydrogen bonding of the histidine imidazole N–H, and nonbonded interactions within the heme binding pocket, the desired orientation of ligands in model hemes must be achieved either by covalent attachment or by crowding to produce nonplanar porphyrin rings. It is commonly observed that meso-only-substituted porphyrins with bulky substituents (mesityl or isopropyl, for example) adopt mainly ruffled geometries² whereas octaalkyltetraphenylporphyrins, OATPPs, adopt mainly saddled conformations because of the steric interaction between adjacent phenyl and alkyl substituents.²

Nonplanar metalloporphyrin complexes undergo the following dynamic processes in solution, (a) ring inversion, (b)

rotation of peripheral substituents (phenyl, ethyl, or other groups), (c) axial ligand exchange, and (d) axial ligand rotation; in the free-base porphyrins, NH tautomerism can be added to this list. Ring inversion is the main focus of this article, and this process is described and studied to the fullest extent possible. However, the other types of dynamics typically observed for porphyrins and metalloporphyrins that might contribute to the dynamics observed in this work will be introduced briefly.

The restricted rotation of phenyl rings resulting from steric interaction with neighboring groups (H, alkyl, or aryl) was first reported by Walker and La Mar³ and has been the subject of considerable investigation by Eaton et al.,⁴ Dirks et al.,⁵ and Medforth et al.⁶ using the dynamic NMR approach and full line shape analysis. This method can be used for

- (3) Walker, F. A.; LaMar, G. N. *Ann. N. Y. Acad. Sci.* **1973**, *206*, 328–348.
- (4) (a) Eaton, S. S.; Eaton, G. R. *J. Chem. Soc., Chem. Commun.* **1974**, 605, 576–577. (b) Eaton, S. S.; Eaton, G. R. *J. Am. Chem. Soc.* **1975**, *97*, 3660–3666. (c) Eaton, S. S.; Eaton, G. R. *J. Am. Chem. Soc.* **1977**, *99*, 6594–6599.
- (5) Dirks, J. W.; Underwood, G.; Matheson, J. C.; Gust, D. *J. Org. Chem.* **1979**, *44*, 2551–2555.
- (6) Medforth, C. J.; Haddad, R. E.; Muzzi, C. M.; Dooley, N. R.; Jaquinod, L.; Shyr, D. C.; Nurco, D. J.; Olmstead, M. M.; Smith, K. M.; Ma, J.-G.; Shelnut, J. A. *Inorg. Chem.* **2003**, *42*, 2227–2241.

* To whom correspondence should be addressed. E-mail: awalker@u.arizona.edu.

(1) Walker, F. A. *Chem. Rev.* **2004**, *104*, 589–615 and references therein.
(2) Scheidt, W. R.; Lee, Y. J. *Struct. Bonding* **1987**, *64*, 1–70.

metalloporphyrin complexes with only one axial ligand³ or with two different axial ligands that cause nonequivalence of the phenyl-*o* and -*m* protons. Coalescence of these phenyl resonances has been observed, and rotational barriers have been calculated for a variety of complexes.^{3,4} In the case of free-base porphyrins, substitution of the ortho and/or meta positions is required for detection of phenyl rotation.^{5,6} Temperature-dependent NMR spectra attributable to phenyl ring rotation have been observed for the Ge, In, Fe, Ru, and Ti complexes of TPP, *p*-*i*-PrTPP, and *p*-CF₃TPP.⁴ The estimated ΔG^\ddagger increases in the order PGe(OH)L \approx PTiO \approx PFeCl < PInCl < PRu(CO) and is 65.2–77.8 kJ mol⁻¹ at their individual coalescence temperatures.⁴ The barrier to phenyl rotation was calculated for free bases, dications, and metal complexes of TArP, TArOPP, OArP, DPP, and DiArPP.^{5,6} It was found that the presence of methyl, fluorine, or methoxy substituents in the phenyl-*o* positions increases the steric interaction with the pyrrole hydrogens and greatly increases the activation energy for phenyl rotation.^{3–6} Phenyl-*p* substituents, on the other hand, have purely electronic effects on the phenyl rotation, with electron-donating groups (Et₂N⁻) causing an order-of-magnitude faster phenyl rotation than electron-withdrawing groups (-CF₃).^{4c} Metal ions have large effects on phenyl ring rotation because of their contribution to the conformation of the porphyrin ring and its possible changes in geometry. The NMR results support the idea that the deformability of the macrocycle is an important factor in controlling the phenyl rotational barriers: ruffling lowers the *meso*-aryl rotational barriers in TArP and TArOPP by moving the *meso* positions out of the porphyrin plane, and saddling (which moves the pyrrole- β positions out-of-plane) appears to lower the barriers for β -aryl rotation in OArP.^{5,6} Therefore, the saddled complexes of this study with phenyl groups on the *meso* carbons are expected to have very high barriers for phenyl rotation, such that this process is too slow to influence the NMR behavior (line shape or volume of NOESY/EXSY cross-peaks) of the complexes under the conditions described below. On the other hand, it has been shown that H₂OETPP and its metal complexes have very low barriers to ethyl group rotation,⁷ such that this process is very fast on the NMR time scale and is not rate-determining for the study of porphyrin ring inversion. In short, of the two types of substituents, we expect the *meso*-phenyl rotation to be a very high energy process in metal OATPP complexes and the β -ethyl rotation to be a very low energy process in metal OETPP complexes, and thus, neither of these substituent effects will interfere with our intended study of porphyrin ring inversion.

Axial ligand exchange (dissociation of bound ligand and binding of free ligand) is a first-order process in six-coordinate Fe^{III} porphyrinates⁸ indicating a dissociative mechanism. Nevertheless, if the concentration of the axial ligand is not sufficient to form the complex to an overwhelming extent ([M complex]/[M starting material] \geq 100), as governed by the equilibrium constant, a measurable

concentration of the intermediate in the complex formation equation will certainly contribute to the observed rapid axial ligand exchange, as well as to line broadening of porphyrin resonances. The five-coordinate intermediate is typically high-spin and has broader signals than the low-spin six-coordinate product of most bis-ligand complex formations or even than those of the $S = 3/2$ bis-ligand complex, [FeOETPP(4-CNPpy)₂]⁺.⁹ Rates of axial ligand exchange can be determined by using 1D ¹H NMR (DNMR) line shape analysis of the axial ligand resonances in the regime of fast ligand exchange or by measuring the volumes of the cross-peaks between the free and bound ligand in 2D NOESY/EXSY (nuclear Overhauser and exchange spectroscopy/exchange spectroscopy) spectra. For the complexes in the present study, except for [FeOETPP(*t*-BuNC)₂]ClO₄, the averaged single resonance for the free and bound ligand was not detected in the NMR spectra in the temperature range studied. In contrast, separate resonances for free and bound ligand were present, and the cross-peaks between them were observed in the 2D NOESY/EXSY spectra of every complex. Cross-peaks disappeared at temperatures from -20 to -80 °C depending on the axial ligand and porphyrin substituents, and the studies of ring inversion described below have been carried out in the regime of slow or “no” axial ligand exchange. In the special case of [FeOETPP(*t*-BuNC)₂]ClO₄, the coalescence temperature for ligand exchange, 0 °C, as well as the ΔG^\ddagger_{273} value of 49.3 kJ mol⁻¹, is the lowest of all of the complexes studied, and the axial ligand exchange rate at that temperature (2.0×10^3 s⁻¹) is the highest observed.

In model complexes, in contrast to proteins, axial ligand rotation is generally assumed to be fast on the NMR time scale at ambient temperatures, as axial ligands of model complexes are not constrained by the protein environment. NMR investigations of low-spin Fe(III) porphyrins have confirmed that, even in the case of hindered imidazoles (2-methyl-,^{10–12} 2-ethyl-, and 2-isopropylimidazole;¹³ 1,2-dimethylimidazole;^{10,13} and benzimidazole¹³) or pyridines,¹⁴ ligand rotation is fast at room temperature (for example, the molecular-mechanics-calculated ΔG^\ddagger value is low and equals 9.2 kJ mol⁻¹ for both [FePorphine(Py)₂]⁺ and [FeTPP(Py)₂]⁺ and 3.8 kJ mol⁻¹ for [FeTMP(4-Me₂NPy)₂]⁺) and is accompanied by porphyrin ring inversion. Therefore, the measured rate and activation parameters include contributions from both processes.

In strongly nonplanar model heme complexes, ligand rotation must be accompanied by saddle or ruffle “inversion” of the porphyrin core itself where the atoms displaced above the mean porphyrin plane become displaced below it upon

- (9) Yatsunyk, L. A.; Walker, F. A. *Inorg. Chem.* **2004**, *43*, 757–777.
 (10) Nakamura, M.; Groves, J. T. *Tetrahedron* **1988**, *44*, 3225–3230.
 (11) Walker, F. A.; Simonis, U. *J. Am. Chem. Soc.* **1991**, *113*, 8652–8657.
 (12) Shokhirev, N. V.; Shokhireva, T. Kh.; Polam, J. R.; Watson, C. T.; Raffii, K.; Simonis, U.; Walker, F. A. *J. Phys. Chem. A* **1997**, *101*, 2778–2786.
 (13) Nakamura, M.; Tajima, K.; Tada, K.; Ishizu, K.; Nakamura, N. *Inorg. Chim. Acta* **1994**, *224*, 113–124.
 (14) Safo, M. K.; Walker, F. A.; Raitsimring, A. M.; Walters, W. P.; Dolata, D. P.; Debrunner, P. G.; Scheidt, W. R. *J. Am. Chem. Soc.* **1994**, *116*, 7760–7770.

(7) Medforth, C. J.; Shelnut, J. A. Unpublished results, Davis, CA, 2001.

(8) La Mar, G. N.; Walker, F. A. *J. Am. Chem. Soc.* **1972**, *94*, 8607–8608.

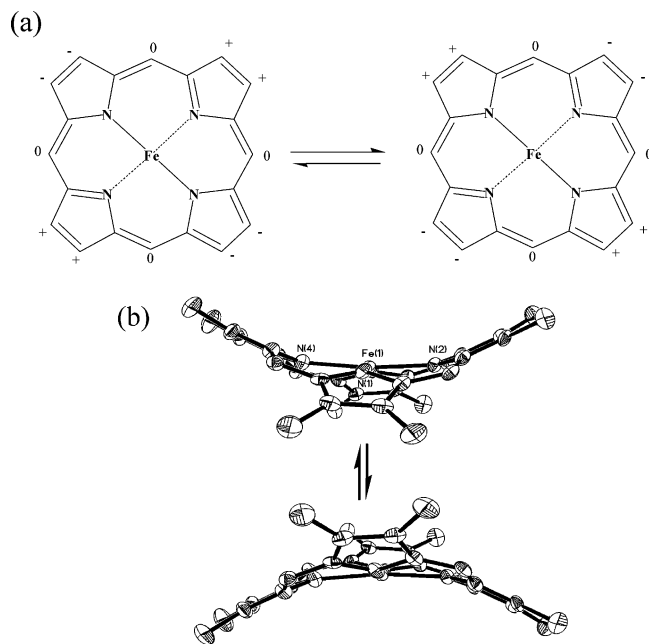


Figure 1. Representation of the macrocycle inversion process for the saddle structure of a porphyrin. (a) Displacements of the atoms with respect to the porphyrin mean plane are shown as + above the plane, - below the plane, and 0 in the plane. (b) Ring inversion approximated using the ORTEP plot generated from the crystal structure of [FeOMTPP(2-MeImH)₂]Cl.²⁷ Phenyl ring and axial ligands have been omitted for clarity. Ring inversion results in the exchange between methyl (for OMTTP) or methylene (for OETTP, F₂₀OETTP, and TC₆TPP) protons.

inversion and vice versa, as shown in Figure 1. If we want to understand the model systems to the fullest extent, this dynamic process, which has no counterpart in heme proteins, must be studied and fully characterized. Saddle- and ruffle-distorted porphyrins invert in a manner that is analogous to cyclohexane chair–chair interconversion.^{15,16} Such inversion has been observed in free-base H₂OMTPP,¹⁷ H₂OETPP,¹⁷ H₂DPP,¹⁸ ZnOETPP,¹⁷ [Co^{III}OETPP(L)₂]⁺ (L = Py, 3-PhPy, 3-ClPy, 1-MeIm, 4-PhImH),^{19,20} the H₄TC₅TPP²⁺ dication,²¹ different Ni(II) porphyrin complexes,^{18,21} (OMTPP)FeCl,²² and (OETPP)FeCl,²² as well as in metal complexes of tetraarylporphyrins with appropriate steric factors for distorting the macrocycle.^{11,12,23–26} The existence of the saddle

inversion in [FeOETPP(1-MeIm)₂]⁺ and [FeOETPP(4-Me₂-NPy)₂]⁺ has been observed qualitatively,²⁷ but quantitative measurements of the rate constants and kinetics parameters as a function of temperature for these complexes had not yet been explored when this work was undertaken. In most of the cases cited above, only coalescence-temperature-determined values were used to characterize the kinetics of ring inversion by applying the standard equations. Thus, unfortunately, for many of these systems, the rate constants and ΔG^\ddagger values for ring inversion are known for one temperature only, and that temperature, in general, differs for each of the porphyrins studied (at a given magnetic field strength).

Ring inversion in nonplanar porphyrins, including the saddled octaalkyltetraphenylporphyrinatoiron(III) complexes of this study i.e., (OMTPP)Fe^{III}, (OETPP)Fe^{III}, (F₂₀OETPP)Fe^{III}, and (TC₆TPP)Fe^{III}, is a symmetrical two-site exchange process (Figure 1) with equal population of the two sites. The rate of ring inversion is comparable to the NMR time scale and can be studied by dynamic 1D ¹H NMR (DNMR) methods above the coalescence temperature of the resonances of the two exchanging species or by 2D NOESY/EXSY techniques at lower temperatures where the two chemical environments are clearly resolved. The rates of ring inversion for two complexes related to this study, (OMTPP)FeCl and (OETPP)FeCl, have already been characterized to some extent by Cheng et al.²² In the case of five-coordinate (OMTPP)FeCl, a single methyl resonance is observed near room temperature and two below the coalescence point, -30 °C, probably measured at 200 MHz.²² The two resonances correspond to the methyl groups *syn* and *anti* to the chloride anion that is coordinated to the iron. This temperature dependence suggests that (OMTPP)FeCl undergoes fast ring inversion with an estimated free energy of activation, ΔG^\ddagger_{243} , of 42.3 kJ mol⁻¹.²² Unfortunately, when two like axial ligands are present, the symmetry of the complex is raised, and no information about ring inversion can be acquired because all eight methyl groups become chemically and magnetically equivalent. In this sense, the metal complexes of both OETPP and TC₆TPP present more interesting cases in which ring inversion can be studied for both five- and six-coordinate complexes because of the presence of diastereotopic geminal methylene protons. Because of the higher distortion of the porphyrin core in (OETPP)FeCl as compared to that of (OMTPP)FeCl,²² the flexibility of the former is lower, and even at room temperature, there are four peaks corresponding to the methylene protons of the ethyl substituents. Diastereotopic methylene protons in five-coordinate iron octaalkyltetraphenyl porphyrins with a saddled geometry should give two peaks corresponding to the “up” or *syn* (toward the chloride ligand) and “down” or *anti* (away from the chloride ligand) positions of the methylene groups. Limited ring

- (15) Medforth, C. J.; Hobbs, J. D.; Rodriguez, M. R.; Abraham, R. J.; Smith, K. M.; Shelnut, J. A. *Inorg. Chem.* **1995**, *34*, 1333–1341.
 (16) Jensen, F. R.; Noyce, D. S.; Sederholm, C. H.; Berlin, A. J. *J. Am. Chem. Soc.* **1960**, *82*, 1256.
 (17) Barkigia, K. M.; Berber, M. D.; Fajer, J.; Medforth, C. J.; Renner, M. W.; Smith, K. M. *J. Am. Chem. Soc.* **1990**, *112*, 8851–8857.
 (18) Medforth, C. J.; Senge, M. O.; Smith, K. M.; Sparks, L. D.; Shelnut, J. A. *J. Am. Chem. Soc.* **1992**, *114*, 9859–9869.
 (19) Medforth, C. J.; Muzzi, C. M.; Smith, K. M.; Abraham, R. J.; Hobbs, J. D.; Shelnut, J. A. *J. Chem. Soc., Chem. Commun.* **1994**, 1843–1844.
 (20) Medforth, C. J.; Muzzi, C. M.; Shea, K. M.; Smith, K. M.; Abraham, R. J.; Jia, S.; Shelnut, J. A. *J. Chem. Soc., Perkin Trans.* **1992**, *2*, 833–837.
 (21) Medforth, C. J.; Berber, M. D.; Smith, K. M.; Shelnut, J. A. *Tetrahedron Lett.* **1990**, *31*, 3719–3722.
 (22) Cheng, R.-J.; Chen, P.-Y.; Gau, P.-R.; Chen, C.-C.; Peng, S.-M. *J. Am. Chem. Soc.* **1997**, *119*, 2563–2569.
 (23) Nakamura, M.; Ikeue, T.; Neya, S.; Funasaki, N.; Nakamura, N. *Inorg. Chem.* **1996**, *35*, 3731–3732.
 (24) Momot, K. I.; Walker, F. A. *J. Phys. Chem. A* **1997**, *101*, 2787–2795.

- (25) Polam, J. R.; Shokhireva, T. Kh.; Raffii, K.; Simonis, U.; Walker, F. A. *Inorg. Chim. Acta* **1997**, *263*, 109–117.
 (26) Momot, K. I.; Walker, F. A. *J. Phys. Chem. A* **1998**, *102*, 10682–10688.
 (27) Ogura, H.; Yatsunyk, L.; Medforth, C. J.; Smith, K. M.; Barkigia, K. M.; Renner, M. W.; Melamed, D.; Walker, F. A. *J. Am. Chem. Soc.* **2001**, *123*, 6564–6578.

inversion at relatively low temperatures lowers the symmetry further and doubles the number of peaks. In the case of (OETPP)FeCl, the four peaks are “inner-up”, “inner-down”, “outer-up”, and “outer-down” (inner and outer, for an adjacent pair of ethyl groups, designates methylene protons that point toward each other and away from each other toward the phenyl rings, respectively).

Ring inversion, in the situation where the ethyl group rotation barrier is low,⁷ leads to rapid rotation of ethyl groups and, as a consequence, to the interchange between inner-up and outer-down and between inner-down and outer-up. Upon warming, the four methylene peaks of (OETPP)FeCl become broader, and coalesce at about 100 °C at 300 MHz.²² The coalescence temperature, T_C , can be used to estimate the rate of ring inversion and the free energy at that temperature according to the standard equations^{28–30}

$$k_{\text{ex}} = \frac{\pi(\Delta\nu)}{\sqrt{2}}$$

$$\frac{\Delta G^\ddagger}{RT_C} = 22.96 + \ln \frac{T_C}{\Delta\nu} \quad (1)$$

where $\Delta\nu$ is the difference in chemical shift between the exchanging species (in Hz) extrapolated to T_C , which can be obtained easily from the corresponding Curie plot. The calculated value of ΔG^\ddagger_{373} for saddled (OETPP)FeCl is 66.1 kJ mol⁻¹,²² which is very close to the value obtained for five-coordinate (OETPP)Zn(Py) at a somewhat lower temperature ($\Delta G^\ddagger_{345} = 67.8$ kJ mol⁻¹)¹⁷ and significantly higher than the value for (OMTPP)FeCl at a much lower temperature ($\Delta G^\ddagger_{243} = 42.3$ kJ mol⁻¹).²² However, the kinetics parameters (ΔH^\ddagger and ΔS^\ddagger) cannot be obtained using only the data for the coalescence temperature; also, the comparison of ΔG^\ddagger for different complexes is difficult because of the differences in the temperature at which ΔG^\ddagger was reported. Therefore, more detailed NMR data and analysis are required. In this work, the full temperature dependence of porphyrin ring inversion and, where present, the concomitant rotation of planar axial ligands have been investigated for various ligand complexes of (OMTPP)Fe^{III}, (OETPP)Fe^{III}, (F₂₀-OETPP)Fe^{III}, and (TC₆TPP)Fe^{III}. The results are compared to those of the meso-only-substituted porphyrin complexes investigated by the NOESY/EXSY methods earlier in this laboratory^{12,24–26} in an effort to understand the differences in the energy barriers and rates of inversion/rotation for highly saddled and highly ruffled metalloporphyrinates.

Experimental Section

All compounds used in this study and their NMR samples were prepared as described in the accompanying article.³¹

- (28) Pople, J. A.; Schneider, W. G.; Bernstein, H. J. *High-Resolution Nuclear Magnetic Resonance*; McGraw-Hill: New York, 1959.
- (29) Oki, M. *Applications of Dynamic NMR Spectroscopy to Organic Chemistry*; VCH: Deerfield Beach, FL, 1985.
- (30) Abraham, R. J.; Fisher, J.; Loftus, P. *Introduction to NMR Spectroscopy*; Wiley and Sons: Chichester, U.K., 1988.
- (31) Yatsunyk, L. A.; Shokhirev, N. V.; Walker, F. A. *Inorg. Chem.* **2005**, *44*, 2848–2866.

NMR Spectroscopy. Most of the work presented herein was carried out on a Varian Unity-300 NMR spectrometer operating at 299.957 MHz ¹H frequency and equipped with a broad-band inverse probe [¹H inner coil and X (¹³C) outer coil] and a Varian variable-temperature unit. The temperature was calibrated using the standard Wilmad methanol sample. A Bruker DRX-500 NMR spectrometer was used only for ambient- to high-temperature experiments because the gradient probes cannot be cooled lower than -20 °C. ¹H 1D spectra were referenced to the residual solvent peak (CD₂Cl₂, 5.32 ppm; CDCl₃, 7.24 ppm; C₂D₂Cl₄, 5.91 ppm; and DMF-*d*₇, 8.02 ppm). All 2D spectra were referenced to specific signals in the 1D spectra.

NOESY/EXSY spectra were acquired at a number of temperatures between -90 and +70 °C depending on the sample, using standard pulse sequences with 512 complex points in the directly detected dimension and 128 t_1 increments in the indirectly detected dimension (states mode). The probe coil was tuned to the proton frequency; the pulse width of the 90° proton pulse and the relaxation time, T_1 , of each proton signal in the 1D ¹H spectrum were determined at each temperature before the 2D experiments were run. The mixing time in the NOESY experiments was set to match the T_1 value of the exchanging protons (methylene protons in OETPP, F₂₀OETPP, and TC₆TPP or methyl protons in OMTPP). Selection of the correct mixing times was crucial: the quantity $\tau_m k_{\text{ex}}$ is most sensitive in the range 0.1–3.5, typically 0.4.^{12,32} In comparison, Dimitrov and Vassilev³³ investigated a four-site exchange system by 1D and 2D EXSY spectroscopy and concluded that the optimum mixing time was given by the relationship $\tau_m k_{\text{ex}} \approx 0.6$, which is very close to the values used in this work. The relaxation delays in 2D experiments were set so that the total recycle time was longer than or equal to T_1 of the phenyl-*p* protons, which were typically the slowest-relaxing protons of the complex, or to the average of the T_1 relaxation times of the free-ligand protons. Most 2D experiments were performed two or three times at a given temperature with different mixing times to ensure the reproducibility of the results and to study the dependence of the kinetics of ring inversion on the mixing times used.

NOESY/EXSY data were processed using the VNMR (Unity 300), Xwinnmr (Bruker DRX-500), or Felix software packages with zero-filling to twice the original data size in both dimensions and Gaussian apodization before each of the two Fourier transformations, followed by baseline correction. The volumes of both cross-peaks and both diagonal peaks of the exchanging pair in the 2D NOESY/EXSY spectra were measured and averaged. If one of the symmetry-related pair of diagonal peaks had considerable overlap with nearby signals, it was not used for calculations. The Origin software package was used for plotting and fitting of the kinetics data. The temperature dependences of the chemical shifts of all complexes have been measured and reported in the accompanying article;³¹ Curie plots of all of the complexes are available in that article or its Supporting Information. The accuracy in calculation of k_{ex} is determined by the accuracy of the measurements, the chemical shift differences but not the values of mixing times. Because of the large chemical shift differences between exchanging species for all of the compounds studied, rates at temperatures in the intermediate-exchange region are accurate within 8–10% uncertainty. Uncertainties for k_{ex} near the slow- and fast-exchange limits are 20%.

Chemical Exchange Rates Measured by NMR Spectroscopy. For a two-site chemical exchange that is fast on the NMR time

- (32) Crans, D. C.; Rithner, C. D.; Thiesen, L. A. *J. Am. Chem. Soc.* **1990**, *112*, 2901–2908.
- (33) Dimitrov, V. S.; Vassilev, N. G. *Magn. Reson. Chem.* **1995**, *33*, 739.

scale (above the coalescence temperature where only the averaged chemical environment of the two exchanging species can be detected), the modified Bloch equations can be simplified to the expression^{28–30}

$$k_{\text{ex}} = \frac{\pi(\Delta\nu)^2}{2(W^* - W_0)} \quad (2)$$

where $\Delta\nu$ is the difference in the chemical shift (in Hz) between the two exchanging species extrapolated to temperatures above T_C , W^* is the width at half-height of the exchange-broadened line, and W_0 is the inherent line width at half-height. W_0 is measured either at high temperatures where chemical exchange is extremely fast on the NMR time scale or at very low temperatures in the absence of chemical exchange. The difference in the denominator indicates how much the NMR line was broadened because of the presence of the dynamic process (ring inversion in this case) only, eliminating the influence of increased solvent viscosity at lower temperatures and NMR parameters such as window (multiplier) function, field inhomogeneity, truncation of the FID, and others. In the case of diamagnetic molecules, all values in eq 2 except W^* remain nearly constant as a function of temperature except close to the freezing point of the solvent where the viscosity changes fairly rapidly. However, for paramagnetic complexes, not only W^* but also W_0 and $\Delta\nu$ change with temperature, and all of these changes must be taken into account. The method of line shape analysis above coalescence is called 1D dynamic NMR spectroscopy, or simply DNMR spectroscopy.

Below the coalescence temperature, where the two different chemical environments are clearly resolved into two NMR resonances, 2D NOESY experiments (also known as EXSY, exchange spectroscopy, when NOESY mixing times are adjusted to match the rate of the exchange process) can be utilized to obtain information about ring inversion. The rate constants, which are proportional to the volumes of the cross-peaks, can be calculated from the equation^{28,34}

$$k_{\text{ex}} = \frac{I_{\text{cross}}}{(I_{\text{cross}} + I_{\text{diag}})\tau_m} \quad (3)$$

where I_{diag} and I_{cross} are the volume intensities of the diagonal and cross-peaks, respectively, and τ_m is the mixing time used in the NOESY experiment. In the special case of two-site exchange with equal-intensity signals, the following equation can be used for the calculation of the rate constant

$$k_{\text{ex}} = \frac{1}{2\tau_m} \ln \left(\frac{I_{\text{diag}} + I_{\text{cross}}}{I_{\text{diag}} - I_{\text{cross}}} \right) \quad (4)$$

Equation 4 is derived from the modified Bloch equations under the assumption that $T_{1A} = T_{1B}$ (where T_{1A} and T_{1B} are the relaxation times for lines A and B of the two exchanging species)³⁵ and is more accurate than the widely used approximation, eq 3, especially when τ_m is relatively long.^{35,36}

The rate constants thus obtained from either DNMR or NOESY/EXSY experiments were used for the determination of the ring

inversion activation parameters, ΔH^\ddagger and ΔS^\ddagger .¹² The dependence of $\ln(k_{\text{ex}}h/k_B T)$ on inverse temperature, or the Eyring plot, was constructed for each complex, and the least-squares linear regression fitting was applied. The slope and intercept of the linear fit were assigned to ΔH^\ddagger and ΔS^\ddagger , respectively, according to the equation^{28–30}

$$\ln \frac{k_{\text{ex}}h}{k_B T} = -\frac{\Delta H^\ddagger}{RT} + \frac{\Delta S^\ddagger}{R} \quad (5)$$

where h is Planck's constant, k_B is the Boltzmann constant, T is the absolute temperature, and R is the gas constant. From these parameters, the free energy of activation, ΔG^\ddagger , and the rate constant for ring inversion, k_{ex} , can be obtained at any temperature.

The Temperature-Dependent Fitting Program, TDFw, was created in this laboratory and used to fit the expanded Curie law dependence of chemical shift on inverse temperature in the fairly common cases of curved dependence that result from the presence of a thermally accessible excited state.^{31,37} The program itself can be downloaded from the Web site <http://www.shokhirev.com/nikolai/programs/prgsciedu.html>; for most of the systems studied in this work in terms of ring inversion kinetics, the temperature-dependent fitting of chemical shifts has already been carried out, and the results are presented in ref 31 or its Supporting Information.

Results

In this work kinetics studies were performed on the five-coordinate nonplanar chloroiron(III) complexes of OMTTP, OETPP, F₂₀OETPP and the perchlorate complex of OMT-PPFe^{III}. The data for (TC₆TPP)FeCl are presented elsewhere.³⁸ The presence of the axial chloride or perchlorate lowers the symmetry of the complexes and creates two different chemical environments for methyl or methylene groups, pointing up toward the chloride and down away from the chloride. When the anion was replaced by two Lewis bases, the symmetry of the complexes was raised, and the kinetics of the bis-ligated OMTTPs could not be studied because of the magnetic equivalence of all eight methyl groups. However, OETPP, TC₆TPP, and F₂₀OETPP porphyrins have diastereotopic methylene protons that were used as probes for ring inversion even in the bis-ligated complexes.

(OMTTP)FeCl Studied by DNMR and 2D NOESY/EXSY Methods. As mentioned above, some basic studies of ring inversion in (OMTTP)FeCl were reported by Cheng et al.²² We have extended these studies over a wide temperature range to determine the activation parameters ΔH^\ddagger and ΔS^\ddagger for this process. In the variable-temperature 1D 300 MHz ¹H NMR studies reported herein, the single methyl resonance observed at ambient temperature broadens upon cooling and splits into two resonances below the coalescence point, T_C , as shown in Figure 2. In the region of the coalescence temperature, spectra were acquired every 2 °C. The precise value of T_C obtained, -26 °C, is close to that reported by Cheng et al.²² (-30 °C), with the small disagreement probably being due to differences in spectrometer temperature calibration. Such a convenient value of T_C presented a unique opportunity to study the ring inversion

(34) Ernst, R. R.; Bodenhausen, G.; Wokaun, A. *Principles of Nuclear Magnetic Resonance in One and Two Dimensions*; Clarendon Press: Oxford, U.K., 1992; Chapter 9.

(35) Jeener, J.; Meier, H.; Bachmann, P.; Ernst, R. P. *J. Chem. Phys.* **1979**, *71*, 4546–4553.

(36) Orrell, K. G. In *Encyclopedia of Nuclear Magnetic Resonance*; Grant, D. M., Harris, R. K., Eds.; Wiley & Sons: Chichester, U.K., 1996; Vol. 8, pp 4850–4857.

(37) Shokhirev, N. V.; Walker, F. A. *J. Phys. Chem.* **1995**, *99*, 17795–17804.

(38) Yatsunyk, L. A.; Walker, F. A. *J. Porphyrins Phthalocyanines* **2005**, in press.

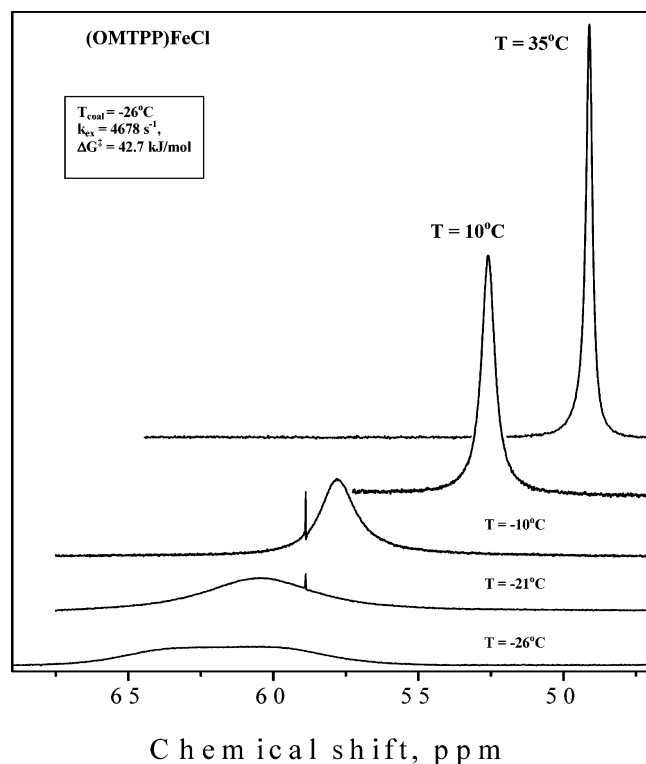


Figure 2. Stacked ^1H 300-MHz NMR spectra (downfield region only) that show broadening of the methyl signal in (OMTPP)FeCl with decreasing temperature. The intensity of all resonances is on a common scale.

of (OMTPP)FeCl by both DNMR and 2D NOESY/EXSY techniques.³⁵

First, the rate and free energy of activation of ring inversion in (OMTPP)FeCl was calculated from the coalescence temperature using eq 1. From the expanded (two-level) Curie plot (Figure 7 of ref 31), the difference in chemical shift for the two methyl protons extrapolated to 247 K was obtained, 7.41 ppm (2223 Hz), allowing calculation of the rate constant, $k_{\text{ex}}^{247} = 4.94 \times 10^3 \text{ s}^{-1}$, and the free energy of activation, $\Delta G_{247}^{\ddagger} = 42.7 \text{ kJ mol}^{-1}$. These data are in good agreement with the $\Delta G_{243}^{\ddagger}$ value of 42.3 kJ mol^{-1} reported by Cheng et al.²² However, as was pointed out earlier, we are interested not only in the values of k_{ex} and ΔG^{\ddagger} at a particular temperature but also in the temperature dependence of k_{ex} , which is necessary to obtain the activation parameters ΔH^{\ddagger} and ΔS^{\ddagger} .

Above the coalescence temperature, T_{C} , line shape analysis was carried out according to eq 2 in which the observed line width, W^* , the inherent line width, W_0 (in the absence of chemical exchange), and the difference in the chemical shift between methyl protons, $\Delta\nu$, all change with temperature. In the extreme narrowing limit ($\tau_{\text{c}} \ll 1/\omega_0$, where τ_{c} is the rotational correlation time and ω_0 is the NMR frequency in radians), W_0 is proportional to τ_{c} , which, in turn, is proportional to the viscosity of the solution, η , according to the Stokes–Einstein equation³⁹

$$\tau_{\text{c}} = \frac{4}{3}\pi r^3 \frac{\eta}{k_{\text{B}}T} \quad (6)$$

where r is the molecular radius (assuming spherical shape),

η is the viscosity of the medium at a given temperature, k_{B} is the Boltzmann constant, and T is the absolute temperature. Values of the viscosity of CH_2Cl_2 were obtained from the Chemistry and Physics Handbook, the International Critical Tables, Data Book of the Viscosity of Liquids,⁴⁰ and other sources⁴¹ and are presented in Figure S1A (Supporting Information). Data from different sources agree very well for all temperatures down to $-60 \text{ }^\circ\text{C}$, and even below this temperature the disagreement is not dramatic. For further calculations at lower temperatures, we used the more recent data [$\log \eta = A + B/(C - T)$, with $A = -4.5147$, $B = -316.63$, and $C = 18.104$].⁴⁰ To estimate W_0 , the line width of the methyl resonance of (OMTPP)FeCl was plotted versus $1000\eta/T$, as shown in Figure S2A (Supporting Information). The initial, high-temperature part of this plot represents the dependence of the line width of the extremely fast exchange line on η/T and can be considered as the inherent line width, W_0 . To obtain a better estimate of W_0 , the line width of the two methyl resonances was measured at 183 K, where ring inversion is no longer detectable on the NMR time scale. Interpolation of the data between the regions of extremely fast chemical exchange and no chemical exchange into the regime where chemical exchange becomes measurable on the NMR time scale makes it possible to obtain an empirical analytical expression for W_0 ($79.03 + 4029\eta/T$, $R = 0.99$, where R is the correlation coefficient) and to calculate the difference in line width, $W^* - W_0$. Finally, the difference in chemical shifts, $\Delta\nu$, was determined from the expanded (two-level) Curie plot for the methyl resonances shown in Figure 7 of ref 31. From this plot, the analytical expression for the temperature dependence of the chemical shifts for the two methyl resonances was found to be $\delta_{\text{CH}_3(1)} = 0.07016 \text{ ppm} + 16172.59/T$ ($R = 0.99$) and $\delta_{\text{CH}_3(2)} = 1.57986 \text{ ppm} + 14058.60/T$ ($R = 0.99$). These dependencies were extrapolated to the relatively high temperatures of the DNMR studies, and $\Delta\nu$ at each temperature of the relatively fast but measurable chemical exchange was calculated and converted to hertz for the 300 MHz spectrometer used. It is clear from the Curie plot and from the analytical expressions for $\delta_{\text{CH}_3(1,2)}$ that $\Delta\nu$ is not constant and increases as the temperature decreases.

With all of the necessary information in hand, the rate of chemical exchange, k_{ex} , was calculated utilizing eq 2 for the ring inversion of (OMTPP)FeCl in the temperature range from 10 to $-26 \text{ }^\circ\text{C}$. This gives the upper part of the Eyring plot shown in Figure 3. The activation parameters were determined from linear fitting of the data: $\Delta H^{\ddagger} = 49(1) \text{ kJ mol}^{-1}$ and $\Delta S^{\ddagger} = 23(4) \text{ J mol}^{-1} \text{ K}^{-1}$. These values were used to calculate the rate of ring inversion in (OMTPP)FeCl and the free energy of activation at 25 $^\circ\text{C}$: $k_{\text{ex}}^{298} = 2.6 \times 10^5 \text{ s}^{-1}$ and $\Delta G_{298}^{\ddagger} = 42(2) \text{ kJ mol}^{-1}$. This means that, at room temperature, the porphyrin ring inverts over a quarter of a million times per second.

(39) Evans, J. N. S. *Biomolecular NMR Spectroscopy*; Oxford University Press: Oxford, U.K., 1995; Chapter 6, pp 238–267.

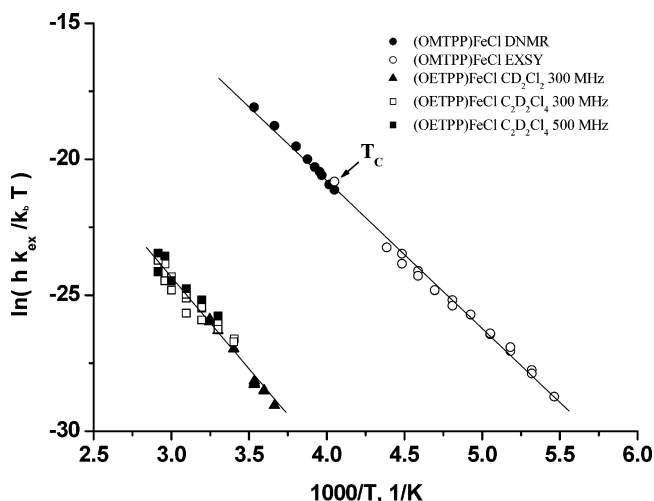
(40) Viswanath, D. S.; Natarajan, G. *Data Book of the Viscosity of Liquids*; Hemisphere Publishing Corporation: Bristol, PA, 1989.

(41) Phillips, T. W.; Murphy, K. P. *J. Chem. Eng. Data* **1970**, *15*, 304–307.

Table 1. Comparison of Activation Enthalpies, Entropies, Room-Temperature Free Energies, and Rate Constants Obtained from the Eyring Plots for Nonplanar Five- and Six-Coordinate Complexes of Iron(III) TC₆TPP, OMTTP, OETPP, and F₂₀OETPP and Several Six-Coordinate TMPFe^{III} and Related Porphyrinates, TMPCo^{III}, and TMPFe^{II} Reported Previously^{12,25}

complex	ΔH^\ddagger (kJ mol ⁻¹)	ΔS^\ddagger (J K ⁻¹ mol ⁻¹)	ΔG_{298}^\ddagger (kJ mol ⁻¹)	k_{ex}^{298} (s ⁻¹) (± 10 –20%)	T range (K)
(TC ₆ TPP)FeONO ₂ ^a	36 ± 1	20 ± 4	30 ± 2	$\geq 3.8 \times 10^7$	183–253
(TC ₆ TPP)FeCl ^a	24 ± 1	-37 ± 3	35 ± 2	$\geq 4.2 \times 10^6$	183–273
(OMTTP)FeCl	45 ± 1	8 ± 3	43 ± 1	2×10^5	183–233
(OETPP)FeCl	56 ± 2	-34 ± 7	66 ± 4	15	273–343
(F ₂₀ OETPP)FeCl ^b	47 ± 1	-52 ± 4	62 ± 2	73	263–303
(OMTTP)FeClO ₄	27 ± 1	-34 ± 4	37 ± 3	$\geq 1.7 \times 10^6$	203–253
[OETPPFe(4-Me ₂ NPY) ₂]Cl	49 ± 1	-22 ± 5	56 ± 3	970	223–263
[F ₂₀ OETPPFe(4-Me ₂ NPY) ₂]Cl	39 ± 1	-56 ± 5	55 ± 3	1.2×10^3	213–253
[TC ₆ TPPFe(4-Me ₂ NPY) ₂]Cl	30 ± 1	-16 ± 6	34 ± 3	$\geq 6.3 \times 10^6$	180–213
[OETPPFe(1-MeIm) ₂]Cl	63 ± 2	12 ± 6	59 ± 3	251	248–278
[TC ₆ TPPFe(4-CNPy) ₂]ClO ₄ ^c	24 ± 4	-20 ± 20	30 ± 10	$\geq 3.8 \times 10^7$	180–193
[OETPPFe(4-CNPy) ₂]ClO ₄ ^c	32 ± 1	-104 ± 3	63 ± 2	59	263–308
[OETPPFe(<i>t</i> -BuNC) ₂]ClO ₄	41 ± 0.4	17 ± 2	36 ± 1	3.0×10^6	180–260
Na[OETPPFe(CN) ₂] ^d	52 ± 2	45 ± 6	39 ± 3	$\geq 1.1 \times 10^6$	220–283
Na[OETPPFe(CN) ₂] ^d	62 ± 2	83 ± 6	37 ± 3	$\geq 2.0 \times 10^6$	236–283
[TMPFe(2-MeImH) ₂]ClO ₄ ^e	51 ± 3	3 ± 15	50 ± 8	1×10^4	213–238
[(2,6-Cl ₂) ₄ TPPFe(2-MeImH) ₂]ClO ₄ ^e	46 ± 4	4 ± 18	45 ± 9	7×10^4	198–218
[(2,6-Br ₂) ₄ TPPFe(2-MeImH) ₂]ClO ₄ ^e	49 ± 2	15 ± 8	44 ± 3	1×10^5	203–223
[TMPCo(4-Me ₂ NPY) ₂]BF ₄ ^f	26	-60	8	1×10^6	188–228
[TMPCo(2-MeImH) ₂]BF ₄ ^e	48 ± 3	-62 ± 11	67 ± 5	14	233–258
[TMPCo(1,2-Me ₂ Im) ₂]BF ₄ ^e	44 ± 5	-84 ± 16	69 ± 10	5	193–253
[TMPFe(1,2-Me ₂ Im) ₂] ^g	~44–51 ^g	0–38 ^h	44–40 ⁱ	~1–6 × 10 ⁵ ^j	183–193

^a Detailed results are presented in ref 38. ^b Data for CD₂Cl₂ solution only. ^c Detailed results are presented in ref 9. ^d In DMF solution. ^e Data taken from ref 12. ^f Data taken from ref 25. ^g Assumed range of ΔH^\ddagger for this complex. ^h Estimated range of ΔS^\ddagger based on k_{ex}^{183} and the assumed range of ΔH^\ddagger . ⁱ Estimated range of ΔG_{298}^\ddagger based on the assumed range of ΔH^\ddagger and the calculated range of ΔS^\ddagger . ^j Estimated range of k_{ex}^{298} .

**Figure 3.** Eyring plot of the kinetics data obtained for porphyrin ring inversion of (OMTTP)FeCl in CD₂Cl₂ (DNMR and NOESY/EXSY) and (OETPP)FeCl in CD₂Cl₂ and C₂D₂Cl₄ (NOESY/EXSY).

Below the coalescence point, the kinetics of ring inversion of (OMTTP)FeCl were studied using the 2D NOESY/EXSY data over the temperature range from -40 to -90 °C. At the lowest temperature, only weak chemical exchange cross-peaks were seen in the 2D NOESY spectrum, suggesting that the rate of ring inversion is not detectable on the NMR time scale below this point at 300 MHz. The mixing times, τ_m , in the NOESY experiments were optimized for the methyl peaks according to their T_1 values ($T_1 \approx 5$ ms in the temperature range from -40 to -90 °C).³¹ The values of τ_m used were on the order of $(0.2 - 2)T_1$, with shorter mixing times (1–5 ms) for higher temperatures (from -40 to -60 °C) and longer mixing times (5–10 ms) for lower temperatures (from -65 to -90 °C). At -40 °C, the rate of chemical exchange was estimated according to eq 3 to be

467 s⁻¹, whereas at -90 °C, it is only 1.3 s⁻¹. Because ring inversion was so much slower at lower temperatures, longer mixing times were required for efficient magnetization transfer. It should be noted that there are experimental constraints on the mixing time itself, based on the relaxation times, T_1 , which become important for investigation of paramagnetic complexes or diamagnetic complexes in which the NMR nucleus studied has short T_1 values. Crans and co-workers have found the optimum mixing times for a four-site ⁵¹V NMR exchange system having fairly short T_1 times, unequal abundances, and multiple rate constants to be in the range of $(0.5 - 1.5)T_1$.³² Thus, it is possible that reaction rates and nuclear T_1 values might be incompatible with the measurement of rate constants in some fast-relaxing systems where extremely short mixing times are required.

The NOESY/EXSY spectra were used to obtain peak volumes and to calculate the rate constants according to eq 3. The second part of the Eyring plot (Figure 3) was then constructed, and activation parameters were obtained by linear fitting: $\Delta H^\ddagger = 40(1)$ kJ mol⁻¹, $\Delta S^\ddagger = -17(4)$ J mol⁻¹ K⁻¹, and $\Delta G_{298}^\ddagger = 45(2)$ kJ mol⁻¹. Data from both DNMR and NOESY/EXSY experiments are in good agreement with each other, so the activation parameters for (OMTTP)FeCl were determined by least-squares linear fitting of the two data sets together; the results are presented in Table 1: $\Delta H^\ddagger = 45(1)$ kJ mol⁻¹ and $\Delta S^\ddagger = 8(3)$ J mol⁻¹ K⁻¹. These values predict that ΔG_{298}^\ddagger is 43(1) kJ mol⁻¹ and the rate of ring inversion is 1.9×10^5 s⁻¹ at 25 °C, close to the quarter of a million value quoted above that was determined from the high-temperature data only.

(OETPP)FeCl Studied by NOESY/EXSY Techniques. Kinetics studies of ring inversion in (OETPP)FeCl were conducted at different magnetic field strengths (300 and 500

MHz) and in two solvents (CD_2Cl_2 and $1,1,2,2\text{-C}_2\text{D}_2\text{Cl}_4$). Although the rate of ring inversion is expected to be field-independent, it is hard to make any predictions about the influence of solvent on the rate of ring inversion; however, as discussed in the accompanying article,³¹ there is a marked dependence of the chemical shifts of the methylene protons of (OETPP)FeCl on the solvent used (for these two solvents).

At room temperature, four resonances are observed for the methylene protons, indicating a relatively slow ring inversion for the (OETPP)FeCl complex and the necessity of utilizing NOESY/EXSY techniques for the kinetics studies. Below -5°C , ring inversion is too slow on the NOESY time scale at 300 MHz, so that no chemical exchange cross-peaks are observed in the 2D NOESY spectra. Raising the temperature leads to considerable broadening of the four methylene peaks, which coalesce at 102°C . Similar results were obtained by Cheng et al.²² and Schünemann et al.⁴² At temperatures higher than 70°C , the diagonal and cross-peaks are too broad for accurate measurements of the peak volumes. Because of these limitations, NOESY/EXSY NMR studies were conducted in the temperature range from -5 to $+70^\circ\text{C}$ at intervals of 5°C . Mixing times, τ_m , were chosen to be on the order of T_1 for the porphyrin methylene protons and were set in the range of $(0.2\text{--}2)T_1$ as in the previous case. The T_1 values of the methylene protons were estimated to be around 6 ms for relatively low temperatures (from 0 to 30°C , CD_2Cl_2) and 4 ms for higher temperatures (from 40 to 70°C , $\text{C}_2\text{D}_2\text{Cl}_4$). For this reason, mixing times, τ_m , in the range of 1–12 ms were used, with higher τ_m values for lower temperatures, where ring inversion is relatively slow.

The volumes of the cross and diagonal peaks in the NOESY/EXSY 2D spectra were measured and used to determine the temperature dependence of the rate constant, k_{ex} , according to eq 3 and to construct the Eyring plot presented in Figure 3. The results show that the rate constants are both field- and solvent-independent for the field strengths and solvents used, and the data points in the Eyring plot can be described by a single linear dependence. The activation parameters are presented in Table 1: $\Delta H^\ddagger = 56(2)\text{ kJ mol}^{-1}$, $\Delta S^\ddagger = -34(7)\text{ J mol}^{-1}\text{ K}^{-1}$, $\Delta G_{298}^\ddagger = 66(4)\text{ kJ mol}^{-1}$, and $k_{\text{ex}}^{298} = 15\text{ s}^{-1}$. Thus, (OETPP)FeCl is much less flexible than (OMTPP)FeCl, and this is likely due to the higher steric constraints caused by the ethyl substituents on the pyrrole- β positions.

(F₂₀OETPP)FeCl Studied by NOESY/EXSY Techniques. (F₂₀OETPP)FeCl is quite similar in NMR behavior and flexibility to the (OETPP)FeCl complex, indicating only a small influence of the phenyl fluorines on the rate of ring inversion of the porphyrin core. The observation of four methylene signals at room temperature indicates a relatively slow ring inversion in this complex. It was studied in the temperature range from -10 to $+35^\circ\text{C}$ in CD_2Cl_2 and from $+40$ to $+70^\circ\text{C}$ in $\text{C}_2\text{D}_2\text{Cl}_4$. Mixing times, τ_m , in the NOESY experiments (1–7 ms) were again selected to be on the same

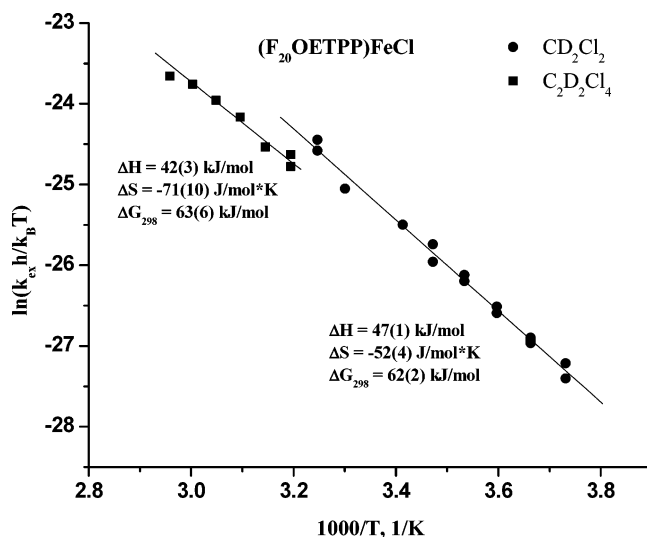


Figure 4. Eyring plot of the kinetics data obtained for porphyrin ring inversion in (F₂₀OETPP)FeCl in CD_2Cl_2 and $\text{C}_2\text{D}_2\text{Cl}_4$ using NOESY/EXSY techniques.

order of magnitude as the T_1 values for the methylene protons (avg $T_1 = 3.7$ ms at 30°C and 3.1 ms at -10°C). For high-temperature measurements ($\text{C}_2\text{D}_2\text{Cl}_4$), experiments were conducted with very short τ_m values of 1–2 ms, but a large spread of the data points was observed, most likely because of the underestimation of the rate when longer mixing times (1.5 and 2 ms) were used; therefore, only rates determined for experiments with $\tau_m = 1$ ms were used for the linear fit. The activation parameters (ΔH^\ddagger and ΔS^\ddagger) obtained from the Eyring plot (Figure 4) differ somewhat for CD_2Cl_2 and $\text{C}_2\text{D}_2\text{Cl}_4$ solvents [$\Delta H^\ddagger = 47(1)\text{ kJ mol}^{-1}$ and $\Delta S^\ddagger = -52(4)\text{ J mol}^{-1}\text{ K}^{-1}$ for CD_2Cl_2 ; $\Delta H^\ddagger = 42(3)\text{ kJ mol}^{-1}$ and $\Delta S^\ddagger = -71(10)\text{ J mol}^{-1}\text{ K}^{-1}$ for $\text{C}_2\text{D}_2\text{Cl}_4$], apparently caused by the different solvation properties of the two solvents. However, the free energies of activation, ΔG_{298}^\ddagger , are within experimental error: 62(2) and 63(6) kJ mol^{-1} for CD_2Cl_2 and $\text{C}_2\text{D}_2\text{Cl}_4$, respectively. On the basis of the least-squares linear fit, the rate of ring inversion at 298 K was estimated to be 73 and 51 s^{-1} for CD_2Cl_2 and $\text{C}_2\text{D}_2\text{Cl}_4$, respectively. Activation parameters for (F₂₀OETPP)FeCl in CD_2Cl_2 are presented in Table 1 and are similar to the corresponding parameters for the (OETPP)FeCl complex, with the ΔH^\ddagger of the fluorinated complex being slightly smaller.

DNMR Studies of (OMTPP)FeClO₄. According to variable-temperature ^1H 1D NMR studies,³¹ one methyl resonance is observed at ambient temperature. It broadens upon cooling and splits into two below the coalescence point, $T_C = -80^\circ\text{C}$. The rate and free energy of activation were first calculated for the coalescence temperature using eq 1. From the extended (two-level) Curie plot,³¹ the difference in chemical shifts for methyl protons extrapolated to -80°C is calculated to be 13.42 ppm (4024 Hz), and therefore, the rate constant, k_{ex}^{193} , is $8.94 \times 10^3\text{ s}^{-1}$ and the free energy of activation, ΔG_{193}^\ddagger , is 32.0 kJ mol^{-1} at the coalescence temperature.

Line shape analysis of the NMR data was carried out in the temperature range from -20 to -70°C according to eq 2. The line width of the methyl resonance was plotted versus

(42) Schünemann, V.; Gerdan, M.; Trautwein, A. X.; Haoudi, N.; Mandon, D.; Fischer, J.; Weiss, R.; Tabard, A.; Guillard, R. *Angew. Chem., Int. Ed.* **1999**, *38*, 3181–3183.

$1000\eta/T$, as shown in Figure S2B ($W_0 = 165.5 + 31865\eta/T$), and $W^* - W_0$ was calculated. The difference in chemical shifts, $\Delta\nu$, was determined first from the extended (two-level) Curie plot for the methyl resonances. However, the lines for the two methyl resonances appear to intersect as the temperature is increased (more experimental data are required to obtain the precise temperature dependence of the methyl resonances) and thus cannot be used for calculating $\Delta\nu$. Therefore, we decided to use the constant value of $\Delta\nu = 3428$ Hz (the largest line width at a temperature right above the T_C). The activation parameters, ΔH^\ddagger and ΔS^\ddagger , were determined from linear fitting of the data to be $27(1)$ kJ mol⁻¹ and $-34(3)$ J mol⁻¹ K⁻¹, respectively, and are presented in Table 1. These values were used to calculate the rate of ring inversion in (OMTPP)FeClO₄ and the free energy of activation, ΔG^\ddagger , at 25 °C [$k_{\text{ex}} \geq 1.7 \times 10^6$ s⁻¹, and $\Delta G^\ddagger_{298} \approx 37(2)$ kJ mol⁻¹]. Because of the approximations involved, these values should be considered only as estimates.

The rates of ring inversion of (OETPP)FeClO₄ could not be measured by NMR techniques because of the extreme breadth of the methylene proton resonances above -80 °C.

NOESY/EXSY Studies of [FeOETPP(4-Me₂NPY)₂]Cl. Methylene protons of ethyl groups are good probes for studying ring inversion in bis-ligated complexes of Fe^{III}-OETPP. There are two diastereotopic methylene resonances, CH₂(out) and CH₂(in), in the 1D spectra of [FeOETPP(4-Me₂NPY)₂]Cl at any temperature below 0 °C, indicating that ring inversion is relatively slow and NOESY/EXSY techniques are required for kinetics studies. NOESY experiments were conducted in a temperature range from -10 to -60 °C at 5 °C intervals and with 5–80 ms mixing times. Ring inversion becomes undetectable (on the EXSY time scale) below -60 °C and only NOE cross-peaks between the geminal pairs of methylene protons are observed. These could be confused with the chemical exchange cross-peaks at this low temperature (below the NOE crossover point, NOE cross-peaks have the same sign as chemical exchange cross-peaks) and can lead to overestimation of the rates of ring inversion. The ratio of the volumes of the cross-peaks to the volumes of the diagonal peaks was plotted versus temperature, as shown in Figure S3 (Supporting Information). The value of the ratio $V(\text{cross-peak})/V(\text{diagonal peak})$ decreases as the temperature is lowered because of the decrease in k_{ex} , but below -60 °C, the ratio begins to increase as the temperature is further reduced indicating the presence of NOE effects only because NOE cross-peak intensities increase as the temperature is lowered below the NOE crossover point.⁴³ The rate of ring inversion was calculated according to eq 3 using only the data from above -60 °C, and the results were plotted in the form of an Eyring plot, which is included in the summary figure shown in the Discussion section. Least-squares linear fitting resulted in the following activation parameters: $\Delta H^\ddagger = 49(1)$ kJ mol⁻¹, $\Delta S^\ddagger = -22(5)$ J mol⁻¹ K⁻¹, $k_{\text{ex}}^{298} = 970$ s⁻¹, and $\Delta G^\ddagger_{298} = 56(3)$ kJ mol⁻¹ (Table 1).

[FeF₂₀OETPP(4-Me₂NPY)₂]Cl Studied by NOESY/EXSY Techniques. No peak(s) for methylene protons are observed in the 1D ¹H NMR spectra above 20 °C. However, when the temperature is lowered to +10 °C, two broad peaks that sharpen with decreasing temperature appear: the downfield peak was assigned to CH₂(out) and the upfield peak to CH₂(in) by analogy with the [FeOETPP(4-Me₂NPY)₂]Cl complex. NOESY/EXSY techniques were used to measure the rate of ring inversion in [FeF₂₀OETPP(4-Me₂NPY)₂]Cl. Experiments were conducted in the temperature range from -20 to -80 °C at 10 °C intervals, and with 10–70 ms mixing times. Peak volumes were measured and used for the calculation of rates of ring inversion according to eq 3. Data below -70 °C were not used in the linear fitting of the Eyring plot because of the significant contributions of NOE intensity to the cross-peak volumes (≥ 10 –20%). Above -70 °C, the intensity of the ring inversion cross-peaks is substantially higher than the intensity of the NOE cross-peaks, so the overestimation of the volume is insignificant.

The Eyring plot for [FeF₂₀OETPP(4-Me₂NPY)₂]Cl is included in the summary figure shown in the Discussion section. The rate constant for ring inversion at 25 °C along with the activation parameters for this complex and other complexes under study are listed in Table 1. The Eyring plot assisted us in estimating the value for the coalescence temperature for the methylene protons. Because of the large difference in the chemical shift between the diastereotopic methylene protons (8.7 ppm at 0 °C, for example), the averaged peak is very broad to the point that it is not detectable in the 1D NMR spectra above 20 °C. From the expanded two-level Curie plot (Figure S17 in the Supporting Information for ref 31), we estimated $\Delta\nu$ for the methylene protons at 20, 30, 40, and 50 °C and calculated k_{ex} using eq 1. Then, values of $\ln(k_{\text{ex}}h/k_B T)$ were obtained and placed on the Eyring plot. The data for 50 °C fit the Eyring plot best. Therefore, we assumed that the coalescence temperature is 50 °C and used eq 1 to obtain the rate of ring inversion and the free energy of activation for this temperature: $k_{\text{ex}}^{323} = 4.90 \times 10^3$ s⁻¹ and $\Delta G^\ddagger_{323} = 56.5$ kJ mol⁻¹.

An attempt was made to go to higher temperatures to investigate ring inversion by DNMR using the averaged methylene peak. Accordingly, [FeF₂₀OETPP(4-Me₂NPY)₂]Cl was dissolved in 1,1,2,2-C₂D₂Cl₄, and 1D experiments were carried out at temperatures up to +80 °C. At these temperatures, all of the peaks became broad, and no methylene peak appeared because of the rapid ligand exchange and, probably, fast spin equilibrium between the high-spin (HS) and low-spin (LS) states of this complex in the presence of a significant concentration of the five-coordinate intermediate, which is expected to be HS. Therefore, no reliable information could be obtained above 323 K.

[FeTC₆TPP(4-Me₂NPY)₂]Cl Studied by DNMR Methods. Ring inversion in [FeTC₆TPP(4-Me₂NPY)₂]Cl is fast on the NMR time scale, and as a result, one sharp peak for the two magnetically inequivalent CH₂(α) protons is observed at temperatures as low as -50 °C. Upon further lowering of

(43) Neuhaus, D.; Williamson, M. P. *The Nuclear Overhauser Effect in Structural and Conformational Analysis*; VCH: New York, 1989; pp 90–92.

the temperature, this peak broadens (960 Hz at $-93\text{ }^{\circ}\text{C}$) but does not split into two, implying that the coalescence temperature is lower than $-93\text{ }^{\circ}\text{C}$. In the extreme case of slow chemical exchange, two methylene resonances are expected, $\text{CH}_2(\text{axial})$ and $\text{CH}_2(\text{equatorial})$, because of the pseudo-cyclohexene conformation of the rings connected to adjacent pyrrole- β -carbons.

The DNMR method was used to estimate the activation parameters of ring inversion for $[\text{FeTC}_6\text{TPP}(4\text{-Me}_2\text{NPy})_2]\text{-Cl}$. The width at half-height of the $\text{CH}_2(\alpha)$ peak was plotted against $1000\eta/T$ (Figure S2C), and the analytical expression for the inherent line width, W_0 , was obtained from linear fitting of the nearly flat high-temperature part of the graph (from -10 to $-40\text{ }^{\circ}\text{C}$): $W_0 = 10.71 + 2725\eta/T$ ($R = 0.87$). Extrapolation of this line into the regime where ring inversion becomes observable on the NMR time scale allowed us to calculate $W^* - W_0$. However, because the sample cannot be cooled to a low enough temperature to bring the system to the slow- or no-exchange regime, the difference in chemical shift, $\Delta\nu$, of the two no-exchange $\text{CH}_2(\alpha)$ resonances cannot be measured. Therefore, it was first assumed that the minimum $\Delta\nu$ must be at least as large as the maximum line width (960 Hz at 300 MHz, 3.20 ppm) at the lowest achievable temperature, $-93\text{ }^{\circ}\text{C}$. Using eq 2, we calculated the rates of ring inversion and obtained the activation enthalpy and entropy by linear fitting of the DNMR data, $32(1)\text{ kJ mol}^{-1}$ and $-2(6)\text{ J mol}^{-1}\text{K}^{-1}$, respectively. These values predict that, at ambient temperature, the minimum rate of ring inversion is $1.2 \times 10^7\text{ s}^{-1}$. Using a larger value of $\Delta\nu$, for example, 1500 Hz, would lead to a 2.4 times higher rate constant, $3.0 \times 10^7\text{ s}^{-1}$, and an only slightly higher ΔS^\ddagger , $6(6)\text{ J mol}^{-1}\text{K}^{-1}$. It should be remembered, however, that there is a hidden error in this assumption: as was seen for other paramagnetic complexes where two different environments of protons are resolved because of the slow chemical exchange, the value of $\Delta\nu$ is not constant but changes with temperature. To make our assumption more reasonable, we constructed two lines, $\text{CH}_2(\alpha)_1$ and $\text{CH}_2(\alpha)_2$ [$(\delta[\text{CH}_2(\alpha)])_{1,2} = \delta[\text{CH}_2(\alpha)\text{avg}] \pm 3.20/2$], that would project the temperature dependence of diastereotopic methylene protons as reasonably as possible to higher temperatures, intersecting with the line for $\text{CH}_2(\alpha)\text{avg}$ at $1/T = 0$ (Figure S4A, Supporting Information). For fitting, we implemented the TDFw program created by Dr. N. V. Shokhkhirev³¹ (available on the Web site given in the Experimental Section); data for $\delta(\text{CH}_2(\alpha)\text{avg})$ were taken from the expanded (two-level) Curie plot of Figure S18 of ref 31; 3.20 ppm is the largest $\Delta\nu$ found at the lowest temperature. Following the standard procedure described above, the following activation parameters were obtained: $\Delta H^\ddagger = 30(1)\text{ kJ mol}^{-1}$ and $\Delta S^\ddagger = -16(6)\text{ J mol}^{-1}\text{K}^{-1}$ (Table 1). It is interesting to note that the activation parameters obtained for $[\text{FeTC}_6\text{TPP}(4\text{-Me}_2\text{NPy})_2]\text{Cl}$ are very close to the activation parameters of its five-coordinate analogue, $(\text{TC}_6\text{TPP})\text{FeCl}$,³⁸ which suggests that ligand rotation does not add to the barrier for porphyrin inversion in this complex.

[FeOETPP(1-MeIm)₂Cl Studied by NOESY/EXSY Methods. In the previous report on this complex,²⁷ the

highest temperature used for the NOESY measurement was $-30\text{ }^{\circ}\text{C}$, which was deemed to be the optimum temperature for obtaining acceptable resolution for most signals and, at the same time, observing both dipolar (NOE) interactions and chemical exchange. For this report, the NOESY spectra were obtained at a higher temperature range (from -30 to $+10\text{ }^{\circ}\text{C}$). Although most of the peaks were broadened to the point where they were no longer recognizable, the methylene peaks were clearly recognizable even at the highest temperature used here ($+10\text{ }^{\circ}\text{C}$).

Rate constants at different temperatures were calculated using eq 4. Error propagation calculations indicated that the error in the calculated rate constant increased with decreasing temperature. At the lower temperatures, the volumes of the cross-peaks are small, even when long mixing times are used, and therefore, they are difficult to measure accurately. This error propagates into the calculated rate constant (given in Table 1) to yield values on the order of $\pm 20\%$ at the lowest temperatures, but $\pm 10\%$ or somewhat less at intermediate temperatures where the volumes of the cross-peaks are large, and again of the order of $\pm 20\%$ at the highest temperatures, where the volumes of the diagonal peaks are small and more prone to measurement errors. Because the nuclear Overhauser effect (NOE) has a positive sign throughout the temperature range studied (the NOE cross-peaks have a negative phase relative to chemical exchange and diagonal peaks), the effect of an NOE is to decrease the apparent rate constant. The relative contribution from the chemical exchange can be increased by increasing the mixing time, but this is not possible when the chemical exchange is slow: because the absolute sizes of all of the peaks decrease with increasing mixing time, long mixing times destroy all information on the chemical exchange rate. The data at the lowest temperatures, those taken at $-30\text{ }^{\circ}\text{C}$, were not included in the linear regression because they deviated significantly from linearity in the Eyring plot for the reasons discussed.

The enthalpy (ΔH^\ddagger) and entropy (ΔS^\ddagger) of activation were calculated by linear regression on the graph of $\ln(k_{\text{ex}}h/k_B T)$ vs $1/T$, as dictated by eq 5, and are $63(2)\text{ kJ mol}^{-1}$ and $12(6)\text{ J mol}^{-1}\text{K}^{-1}$, respectively, in the temperature range from 248 to 278 K. The magnitudes of the residuals are comparable to the calculated errors.

[FeOETPP(*t*-BuNC)₂ClO₄ Studied by DNMR and NOESY/EXSY Techniques. This is the second example, along with $(\text{OMTPP})\text{FeCl}$, of a complex where ring inversion can be fully characterized by both DNMR and NOESY/EXSY techniques, because of a convenient coalescence temperature of $-55\text{ }^{\circ}\text{C}$.⁴⁴ The values of the rate constants for ring inversion and free energy of activation at T_C were calculated according to eq 1 to be $5.87 \times 10^3\text{ s}^{-1}$ and 37.1 kJ mol^{-1} ($\Delta\nu = 8.81\text{ ppm}$ or 2643 Hz at $-55\text{ }^{\circ}\text{C}$), respectively.⁴⁴

Above T_C , the ring inversion in $[\text{FeOETPP}(t\text{-BuNC})_2]\text{ClO}_4$ was studied by DNMR techniques, and the rate constants were calculated using eq 2 in the temperature range from -10 to $-50\text{ }^{\circ}\text{C}$. The line width of the averaged methylene signal

(44) Yatsunyk, L.; Walker, F. A. *Inorg. Chem.* **2004**, *43*, 4341–4352.

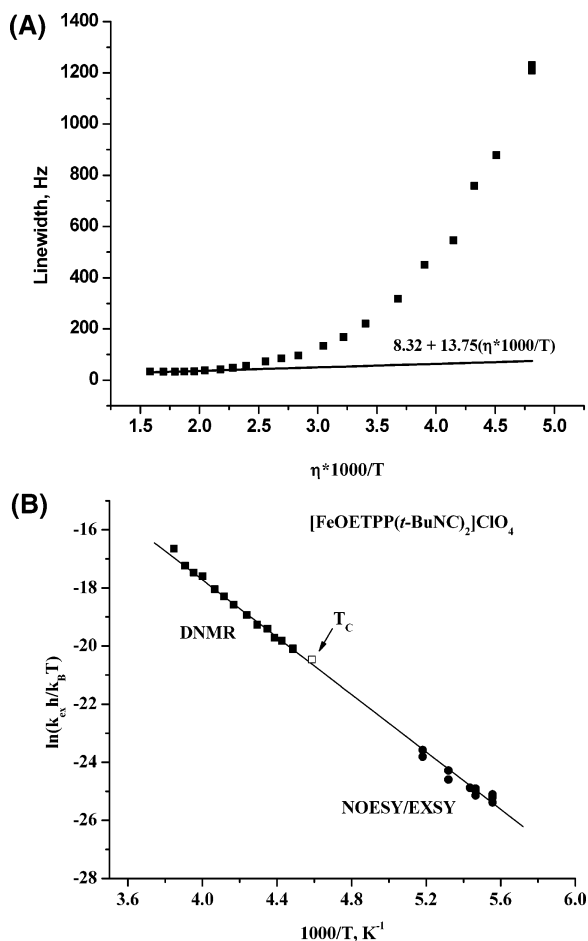


Figure 5. (A) Temperature dependence of the line width, W^* , of the methylene protons in $[\text{FeOETPP}(t\text{-BuNC})_2]\text{ClO}_4$ above the coalescence point (-55°C) showing, extreme line broadening upon cooling. The difference between the straight-line extrapolation of the initial flat part and W^* is attributed to the chemical exchange process involving the inversion of the porphyrin ring. (B) Eyring plot of the kinetics data obtained for porphyrin ring inversion of $[\text{FeOETPP}(t\text{-BuNC})_2]\text{ClO}_4$ in CD_2Cl_2 above (from DNMR spectroscopy) and below (NOESY/EXSY) the coalescence temperature.

was plotted versus $1000\eta/T$ (Figure 5A). The initial, nearly flat, high-temperature part (from $+25$ to -10°C) of this plot was extrapolated to lower temperatures, and $W^* - W_0$ was calculated. The values of $\Delta\nu$ in the temperature range from -10 to -50°C were obtained by linear fitting of the data from the expanded (two-level) Curie plot,³¹ Figure S4B [$\text{CH}_2(\text{out})$, $\delta = -8.69 \text{ ppm} + 4927/T$ ($R = 0.999$); $\text{CH}_2(\text{in})$, $\delta = 1.58 \text{ ppm} + 765/T$ ($R = 0.999$)]. On the basis of these results, $\ln(k_{\text{ex}}/h/k_{\text{B}}T)$ was calculated, and the upper part of the Eyring plot (Figure 5B) was constructed.

Below the coalescence temperature, the kinetics of ring inversion of $[\text{FeOETPP}(t\text{-BuNC})_2]\text{ClO}_4$ were studied using the 2D NOESY/EXSY experiment over the temperature range from -75 to -93°C . The mixing time was set to 1–10 ms (0.02 – $0.2 T_1$), which is much shorter than the relaxation time, T_1 , of the methylene protons, because, even at low temperatures, the ring inversion process is very fast and longer mixing times lead to saturation of the signals and loss of the rate information. By repeating the measurements at 3–4 different mixing times, it was shown that such short mixing times still result in reproducible and consistent data.

The fact that chemical exchange for $[\text{FeOETPP}(t\text{-BuNC})_2]\text{ClO}_4$ is observed even at low temperatures indicates the relatively high flexibility of this complex due to low steric constraints of the $t\text{-BuNC}$ ligands.

The results from NOESY/EXSY spectra were used to calculate the rates of ring inversion according to eq 3 and to build the second half of the Eyring plot (Figure 5B). Data obtained from both DNMR and NOESY/EXSY experiments are in excellent agreement with each other. Therefore, the activation parameters for $[\text{FeOETPP}(t\text{-BuNC})_2]\text{ClO}_4$ were determined from linear fitting of the two data sets together: $\Delta H^\ddagger = 41.0(4) \text{ kJ mol}^{-1}$ and $\Delta S^\ddagger = 17(2) \text{ J mol}^{-1} \text{ K}^{-1}$. These values predict that the free energy of activation, ΔG^\ddagger_{298} , is $36(1) \text{ kJ mol}^{-1}$ and the rate of ring inversion is $3.0 \times 10^6 \text{ s}^{-1}$ at 25°C . The value of ΔG^\ddagger_{298} is close to that for $\text{Na}[\text{FeOETPP}(\text{CN})_2]$ (see below) and reflects the process of ring inversion of the OETPP core, where the metal is in the mean plane of the porphyrin macrocycle and the axial ligands are very small. On the other hand, OETPP complexes with planar aromatic axial ligands have substantially higher ΔG^\ddagger_{298} values (on the order of 60 kJ mol^{-1}) that include ring inversion and ligand rotation activation contributions.

$\text{Na}[\text{FeOETPP}(\text{CN})_2]$ Studied by DNMR Techniques.

Unlike all other bis-ligated iron(III) complexes of OETPP, only one methylene peak appears in the NMR spectra of $\text{Na}[\text{FeOETPP}(\text{CN})_2]$ at all temperatures,³¹ suggesting relatively high rates of ring inversion for this complex in the studied temperature range. 1D ^1H NMR data were acquired from $+80$ to -57°C (mp for $\text{DMF-}d_7$ is -61°C) with 2–5 $^\circ\text{C}$ intervals. The methylene peak is sharp at high temperatures but broadens upon cooling until it disappears almost completely at -57°C , which can be considered as the coalescence temperature, T_c . Using eq 1, the free energy of activation and the rate of ring inversion at the coalescence temperature were found to be $\Delta G^\ddagger_{216} = 39.7 \text{ kJ mol}^{-1}$ and $k_{\text{ex}}^{216} = 1.1 \times 10^3 \text{ s}^{-1}$, respectively. Line shape analysis was carried out according to eq 2 in the same manner as for the other complexes in this study. First, the dependence of the viscosity of DMF upon temperature was determined. Values of viscosity were taken from the Web site of the manufacturer, BASF,⁴⁵ and Data Book of the Viscosity of Liquids.⁴⁰ The former dataset contained data from 153 to -30°C and was fit to a third-order polynomial ($y = A + B_1x + B_2x^2 + B_3x^3$) with the coefficients $A = -7.09 \pm 1.07$, $B_1 = 7.53 \pm 1.00$, $B_2 = -2.66 \pm 0.31$, and $B_3 = 0.33 \pm 0.03$ with $R = 0.9994$. On the other hand, the latter source contained data from 47 to -3°C and was best described with the function $\log \eta = A + B/(C - T)$, where $A = -3.6398$, $B = -56.047$, and $C = 194.25$ (Figure S1B). The values of viscosity from these two sources agree well in the temperature range from $+47$ to -10°C ; however, outside this range, a large discrepancy, especially for the lower temperatures, was observed (Figure S1B). For all of the calculation of kinetics parameters in this work, the first data set was used because it is more recent and contains data from a broader range of temperatures.

(45) http://www.basf.de/Basf/img/produkte/loesemittelle/DMF_e.pdf.

The values of $W^* - W_0$ were calculated from the NMR data and the analytical expression for W_0 ($10.09 + 3677\eta/T$, Figure S2D). Because the sample could not be cooled to the temperatures where two distinct resonances are observed for diastereotopic methylene protons, it was first assumed that the minimum difference in chemical shift, $\Delta\nu$, should be at least as large as the maximum line width, 490 Hz. With this assumption, the rate of ring inversion in the temperature range from 10 to -50 °C was calculated according to eq 2. Least-squares linear fitting of the data resulted in the activation parameters $\Delta H^\ddagger = 58(1)$ kJ mol $^{-1}$ and $\Delta S^\ddagger = 73(6)$ J mol $^{-1}$ K $^{-1}$, which, in turn, gave estimates of the minimum rate of ring inversion (k_{ex}^{298}) and the free energy of activation at 298 K of 2.7×10^6 s $^{-1}$ and 36(3) kJ mol $^{-1}$, respectively. When the temperature range was narrowed to match the range for which the solvent viscosity data are available (from 10 to -37 °C), then the activation parameters obtained were $\Delta H^\ddagger = 68(2)$ kJ mol $^{-1}$, $\Delta S^\ddagger = 112(7)$ J mol $^{-1}$ K $^{-1}$, and $\Delta G^\ddagger_{298} = 35(4)$ kJ mol $^{-1}$, and the minimum rate of ring inversion was $k_{\text{ex}}^{298} = 4.9 \times 10^6$ s $^{-1}$. However, as mentioned above, an error is implemented in the data because of the constant value of $\Delta\nu$ used. The error caused by assuming a constant $\Delta\nu$ in this case is quite large because of the wide temperature range over which the rates were measured. Therefore, as in the case of [FeTC $_6$ TPP(4-Me $_2$ NPY) $_2$]Cl, we took the expanded (two-level) Curie plot of Figure S19 (Supporting Information),³¹ specifically the line for the methylene protons, CH $_2$ (avg), used the largest $\Delta\nu$, 490 Hz, 1.63 ppm; and, using the TDFw program,³¹ constructed two lines, CH $_2$ (1) and CH $_2$ (2) [$\delta(\text{CH}_2(1,2)) = \delta(\text{CH}_2(\text{avg})) \pm 1.63/2$], that intersect the line for CH $_2$ (avg) at $1/T = 0$ (Figure S4C). As a result of this treatment, the following activation parameters were obtained in the temperature range from +10 to -50 °C: $\Delta H^\ddagger = 52(2)$ kJ mol $^{-1}$ and $\Delta S^\ddagger = 45(6)$ J mol $^{-1}$ K $^{-1}$ (Table 1). These values allowed us to calculate the rate of ring inversion and the free energy of activation at room temperature: $\Delta G^\ddagger_{298} = 39(3)$ kJ mol $^{-1}$ and $k_{\text{ex}}^{298} \geq 1.1 \times 10^6$ s $^{-1}$. For the narrower temperature range, from +10 to -37 °C, the following parameters were obtained: $\Delta H^\ddagger = 62(2)$ kJ mol $^{-1}$, $\Delta S^\ddagger = 83(6)$ J mol $^{-1}$ K $^{-1}$, $\Delta G^\ddagger_{298} = 37(3)$ kJ mol $^{-1}$, and $k_{\text{ex}}^{298} = 2.0 \times 10^6$ s $^{-1}$.

Ring inversion in (TC $_6$ TPP)FeCl, [FeOETPP(4-CNPy) $_2$]ClO $_4$, and [FeTC $_6$ TPP(4-CNPy) $_2$]ClO $_4$ was studied by both DNMR and NOESY/EXSY techniques. These experiments and their conclusions are presented in detail elsewhere,^{9,38} but for completeness and comparison, the kinetics parameters are included in Table 1.

Discussion

The activation enthalpies, ΔH^\ddagger ; entropies, ΔS^\ddagger ; and free energies, ΔG^\ddagger_{298} , and the ring inversion rate constants at 298 K for the complexes of this study are summarized in Table 1. The Eyring plots for all systems under investigation and those reported earlier^{9,38} are shown in Figure 6. The kinetics parameters can be interpreted as follows: ΔH^\ddagger indicates the barrier to macrocycle inversion and should thus be a measure of rigidity, and ΔS^\ddagger indicates the gain or loss of order on

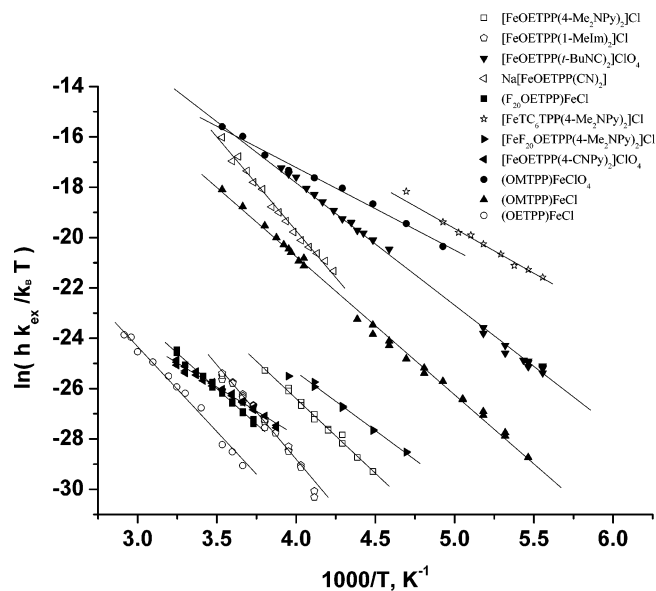


Figure 6. Eyring plot of the kinetics data obtained for porphyrin ring inversion in octaalkyltetraphenyliron(III) five- and six-coordinate porphyrins.

going from the ground to the transition state for ring inversion. The current study is the only one in which ΔH^\ddagger and ΔS^\ddagger of activation of porphyrin inversion in highly saddled porphyrinates of any kind have been reported. We have scrutinized our data for possible systematic errors, for example, by plotting ΔH^\ddagger vs ΔS^\ddagger to see whether there is a linear relationship that would indicate an isokinetic temperature (where all systems studied have the same ΔG^\ddagger).^{46,47} We find no apparent correlation between ΔH^\ddagger and ΔS^\ddagger by metal complex coordination number, porphyrin substituents, or other variables, thus suggesting no obvious systematic error.

The rate constants of ring inversion for different octaalkyltetraphenylporphyrinatoiron(III) complexes at 298 K span a range of 6 orders of magnitude, from 10 to 10^7 s $^{-1}$, indicating a large range of porphyrin core flexibilities. According to the value of k_{ex}^{298} , all of the complexes studied can be placed in one of three groups: (1) (OMTPP)FeClO $_4$ and five- and six-coordinate (TC $_6$ TPP)Fe III complexes for which $k_{\text{ex}}^{298} \approx 10^7$ s $^{-1}$; (2) (OMTPP)FeCl and six-coordinate (OETPP)Fe III complexes with small cylindrical ligands (CN $^-$ and *t*-BuNC) for which $k_{\text{ex}}^{298} \approx 10^5$ – 10^6 s $^{-1}$; and (3) (OETPP)FeCl, (F $_2$ OETPP)FeCl, and their six-coordinate analogues with planar aromatic axial ligands (4-Me $_2$ NPY, 1-MeIm, and 4-CNPy) for which $k_{\text{ex}}^{298} \approx 10$ – 10^3 s $^{-1}$. The deviation of the porphyrin core from planarity, the position of the Fe atom (relative to the porphyrin mean plane), and the barrier to axial ligand rotation appear to dictate the placement of a given complex in a particular group. In our discussion, we intend to address the influence of the following parameters on the porphyrin core kinetics: porphyrin core nonplanarity, axial ligand type, Fe atom position, phenyl substituents, metal type, and solvation effects.

(46) Leffler, J. E. *J. Org. Chem.* **1955**, *20*, 1202–1231.

(47) Lowry, T. H.; Richardson, K. S. *Mechanism and Theory in Organic Chemistry*, 2nd ed.; Harper & Row: New York, 1981; pp 142–145.

Table 2. Average Displacement of Selected Atoms from the Mean Porphyrin Plane in Five-Coordinate Octaalkyltetraphenyliron(III) Chlorides

complex	avg $ \Delta C_{\beta} $ (Å)	avg $ \Delta C_{\text{m}} $ (Å)	$ \Delta \text{Fe} $ (Å) ^a	$\Delta 24$ (Å) ^b	ref
(OETPP)FeCl	± 1.15	± 0.19	0.43	0.58	22
	± 1.13	± 0.22	0.48	0.57	42
(OMTPP)FeCl	± 1.05	± 0.14	0.51	0.53	22
(TC ₆ TPP)FeCl	± 0.66	± 0.47	0.53	0.40	38

^a Deviation of Fe from the mean plane of the 24-atom core. ^b $\Delta 24$ is the average deviation of 24 atoms from the mean porphyrin plane.

First, let us consider only the five-coordinate chloride complexes, (OMTPP)FeCl, (TC₆TPP)FeCl,³⁸ and (OETPP)FeCl, to investigate the influence of porphyrin nonplanarity on the rates of ring inversion. It has been proposed²¹ that the rates of this process are likely to be very sensitive to the degree of steric interactions between the peripheral substituents and might thereby provide an indirect measurement of the degree of nonplanarity of the porphyrin core; a more nonplanar conformation should be accompanied by an increase in the free energy of activation (ΔG^\ddagger) for inversion if entropy considerations are neglected. All three iron chlorides adopt saddled geometries with different degrees of ruffling and nonplanarity in the solid state (Table 2). They can be placed in the following order according to decreasing distortion of their cores: OETPP > OMTPP > TC₆TPP (as seen by the average deviation of the 24 atoms from the mean porphyrin plane, denoted $\Delta 24$).^{22,38,42} In the same order, the free energy of activation decreases [$\Delta G^\ddagger_{298} = 66(4) > 43(1) > 35(2)$ kJ mol⁻¹], and the rate of ring inversion increases ($k_{\text{ex}}^{298} = 15 < 2 \times 10^5 < 4.2 \times 10^6$ s⁻¹). As was mentioned above, ΔH^\ddagger indicates the barrier to ring inversion of the porphyrin core and is higher for (OETPP)FeCl and lower for (TC₆TPP)FeCl because of the substantial nonplanarity of the former and the much smaller degree of nonplanarity of the latter, as shown in Table 2 [$\Delta H^\ddagger = 56(2) > 45(1) > 24(1)$ kJ mol⁻¹]. Now, using the kinetics data for this series of similar porphyrins (octaalkyltetraphenylporphyrinato-iron(III)), we can predict the degree of nonplanarity for a complex whose crystal and molecular structure has not yet been determined. (F₂₀OETPP)FeCl has a slightly larger ΔH^\ddagger value than (OMTPP)FeCl [47(1) vs 45(1) kJ mol⁻¹]; by the same token, it has a slightly smaller ΔG^\ddagger_{298} value [62(2) vs 66(4) kJ mol⁻¹] and a slightly larger k_{ex}^{298} value (75 vs 15 s⁻¹) than (OETPP)FeCl. Therefore, by either measure, (F₂₀-OETPP)FeCl should have a similar but intermediate degree of nonplanar distortion of its core compared to the OMTPP and OETPP complexes. In short, it is evident that porphyrin geometry defines the kinetics of ring inversion, with the least saddled porphyrin cores being the most flexible.

Second, the influence of axial ligands on the kinetics of ring inversion can be assessed by considering the different bis-ligated complexes of (OETPP)Fe^{III}. As previously mentioned, these complexes fall into two different groups with a high rate of ring inversion for the bis-(*t*-BuNC) and bis-(CN⁻) complexes and a relatively low rate of ring inversion (by at least a factor of 10³) for complexes with planar aromatic ligands (4-Me₂NPy, 4-CNPy, and 1-MeIm). ΔG^\ddagger_{298} values are very similar within the group and equal ~ 37 and

~ 59 kJ mol⁻¹ for the first and second groups, respectively. (OETPP)Co^{III} complexes with different imidazoles and pyridines (Py, 3-PhPy, 3-ClPy, 1-MeIm, and 4-PhIm) also have very similar values of ΔG^\ddagger at their coalescence temperatures (51.5–56.1 kJ mol⁻¹) despite the wide variety of aromatic ligands used and their probably somewhat differing, but unstated, coalescence temperatures.¹⁹ Similar values of ΔG^\ddagger_{298} for (OETPP)Fe^{III} complexes with planar aromatic axial ligands can be explained in the following manner. The values of ΔH^\ddagger [63(2) > 49(1) > 32(1) kJ mol⁻¹] and ΔS^\ddagger [12(6) > -22(5) > -104(3) J mol⁻¹K⁻¹] decrease, resulting in a relatively constant value of ΔG^\ddagger_{298} [59(3) \approx 56(3) \approx 63(2) kJ mol⁻¹], only if we arrange the complexes with similar deviations from the mean porphyrin plane ($\Delta 24 = 0.59, 0.62,$ and 0.61 Å) in order of increasing average Fe–N_{ax} distance [1.977(3) < 2.04(1) < 2.22(1) Å] for [OETPPFe(1-MeIm)₂]Cl,⁴⁸ [OETPPFe(4-Me₂NPy)₂]Cl,²⁷ and [OETPPFe(4-CNPy)₂]ClO₄,⁹ respectively. In other words, since ring inversion in bis-ligated (OETPP)Fe^{III} with planar aromatic axial ligands must be accompanied by ligand rotation, lengthened Fe–N_{ax} bonds facilitate ring inversion by decreasing the activation barrier to ligand rotation. Therefore, the kinetics parameters obtained must include contributions from at least two processes, porphyrin ring inversion and axial ligand rotation. In contrast, the latter is not included in the kinetics data for the complexes having cylindrical axial ligands, i.e., the bis-(*t*-BuNC) and bis-(CN⁻) complexes. By comparing the free energy of activation for the two groups of complexes, we can estimate the free energy of axial ligand rotation alone to be roughly 20–25 kJ mol⁻¹ for pyridines and unhindered imidazoles. However, further studies will be required to obtain accurate values.

Comparing the five- and six-coordinate complexes of the same porphyrin, one can see a similarity between the activation parameters for the five-coordinate chlorides and the corresponding bis-(pyridine) or bis-(imidazole) analogues (Table 1), with the five-coordinate complexes being slightly less flexible (higher ΔG^\ddagger_{298}) and having lower rates for ring inversion). The Fe atom in five-coordinate complexes is significantly out of the mean porphyrin plane, by 0.43/0.48, 0.51, and 0.53 Å for (OETPP)Fe^{III}, (OMTPP)Fe^{III}, and (TC₆-TPP)Fe^{III}, respectively (Table 2). This imposes steric hindrance on the ring inversion by increasing the amount of energy necessary for porphyrin ring rearrangement in those five-coordinate complexes and, therefore, results in lower inversion rates. In all six-coordinate complexes, on the other hand, the Fe atom is exactly in the porphyrin mean plane and does not interfere with ring inversion. Therefore, the rearrangement in five-coordinate porphyrin complexes has approximately the same contribution to the activation energy as does the ligand rotation that accompanies the ring inversion in six-coordinate complexes, which fortuitously results in similar activation parameters for these two groups of porphyrin complexes with quite different structural features.

(48) Yatsunyk, L. A.; Carducci, M. D.; Walker, F. A. *J. Am. Chem. Soc.* **2003**, *125*, 15986–16005.

The $(F_{20}OETPP)FeCl$ and $[F_{20}OETPPFe(4-Me_2NPy)_2]Cl$ complexes were observed to have more negative values of ΔS^\ddagger [$-52(4)$ vs $-34(7)$ and $-56(5)$ vs $-22(5)$ $J\ mol^{-1}\ K^{-1}$] and lower values of ΔH^\ddagger [$47(1)$ vs $56(2)$ and $39(1)$ vs $49(1)$ $kJ\ mol^{-1}$] than their $(OETPP)Fe^{III}$ counterparts. This might be a result of more precise requirements for the orientation of the pentafluorophenyl rings during ring inversion. The lower values of ΔH^\ddagger might indicate that the ground state of the $F_{20}OETPPFe^{III}$ complexes is at higher energy and its transition state is of enthalpy similar to that of the $OETPPFe^{III}$ complexes. The presence of larger ortho substituents, either methyls or fluorines, increases the steric interaction with the pyrrole ethyl groups and greatly increases the activation energy of rotation of phenyl rings, as has been shown previously.⁴ However, values of ΔH^\ddagger and ΔS^\ddagger were not reported in the earlier work, so no direct comparison between the results observed in this work and previous studies can be made.

As for the effect of the metal on the kinetics of ring inversion of the OETPP porphyrin core, our data can be compared to the data obtained for a series of $[Co^{III}OETPP(L)_2]^+$ complexes, with $L = Py, 3-PhPy, 3-ClPy, 1-MeIm,$ and $4-PhImH$ (ΔG^\ddagger values at the coalescence temperatures are $52-56\ kJ\ mol^{-1}$);^{19,20} $Zn(II)OETPP(Py)$ [$\Delta G^\ddagger_{345} = 68(1)\ kJ\ mol^{-1}$];¹⁷ $Ni(II)OETPP$ [$\Delta G^\ddagger_{293} = 55(1)\ kJ\ mol^{-1}$];²¹ H_2OETPP [$\Delta G^\ddagger_{383} = 76(1)\ kJ\ mol^{-1}$];¹⁷ and H_4OETPP^{2+} ($\Delta G^\ddagger_{>407} > 84\ kJ\ mol^{-1}$).²¹ Unfortunately, all of the activation parameters were reported for coalescence temperatures only, but because we have the ΔH^\ddagger and ΔS^\ddagger values for some systems related to these, we can calculate the ΔG^\ddagger values at the reported temperatures for direct comparison of our data with the literature data, as is done below.

Some general conclusions regarding the effect of the metal (or protons) can be made. First, free-base H_2OETPP and its dication have high values of ΔG^\ddagger because of the high steric repulsion of the NH protons. Introduction of metal (Fe, Zn, Co, or Ni) decreases the free energy of activation for porphyrin ring inversion by removing the steric strain. Then, complexes that have the metal out of the porphyrin mean plane, $(OETPP)FeCl$ (by $0.43/0.48\ \text{\AA}$)^{22,42} and $Zn(II)OETPP(Py)$ (by $0.22\ \text{\AA}$),¹⁷ have higher values of ΔG^\ddagger [$68(4)$ and $68(1)\ kJ\ mol^{-1}$, respectively, at the coalescence temperature of the $Zn(II)$ complex, $345\ K$] than do complexes where the metal is in the mean porphyrin plane, such as $[OETPPFe(L)_2]^+$ and $[OETPPCo(L)_2]^+$ (where $L =$ various pyridines and imidazoles)^{19,20} and $NiOETPP$,²¹ all with ΔG^\ddagger of about $50-56\ kJ\ mol^{-1}$. However, comparing $Ni(II)OETPP$ to the $[OETPPFe(t-BuNC)_2]^+$ complex of this study, the calculated ΔG^\ddagger_{293} for the latter is $36\ kJ\ mol^{-1}$; if the values for the bis-cyanide complex are used instead, ΔG^\ddagger_{293} is $37.7-38.8\ kJ\ mol^{-1}$. Whereas the comparison between the five-coordinate $Zn(II)$ and $Fe(III)$ complexes at $345\ K$ is good, the comparison between the $Ni(II)$ four-coordinate and $Fe(III)$ six-coordinate OETPP complexes with cylindrical ligands is not; it is not clear whether this represents a true difference in the activation free energy for the different coordination numbers. In one study related to highly ruffled $[TMPPFe(4-CNPy)_2]^+$, it was shown by MM2 calculations

that the TMP complex had a smaller activation enthalpy for ligand rotation than did the corresponding porphine and TPP complexes because of its higher-enthalpy ground state,¹⁴ and this might also be the case for some of the systems of this study. However, for five- and six-coordinate complexes having planar axial ligands, it appears that the nature of the metal itself does not have a large impact on the kinetics parameters; only the conformation of the porphyrin induced by the presence of the metal appears to be crucial.

The final issue to address regarding the $Fe(III)$ complexes of this study is the solvation effect. Whereas the activation parameters for $(OETPP)FeCl$ are field- and solvent-independent, the activation entropy, enthalpy, and free energy of ring inversion in $(F_{20}OETPP)FeCl$ and $[FeOETPP(4-CNPy)_2]^+$ ⁹ are slightly dependent on the nature of the solvent used. Solvation effects can be explained by the difference in coordination abilities of the metalloporphyrin complex by CD_2Cl_2 as compared to $C_2D_2Cl_4$ or $CDCl_3$. To us, the absence of solvation effects in the case of $(OETPP)FeCl$ is more surprising than their presence in the cases of $(F_{20}OETPP)FeCl$ and $[FeOETPP(4-CNPy)_2]^+$. It should also be pointed out that the bis-cyanide complex, $Na[FeOETPP(CN)_2]$, was studied only in dimethylformamide, and thus, we are unable to evaluate solvation effects for this complex.

In comparison to the octaalkyltetraphenylporphyrinato-iron(III) complexes investigated in this work, previous studies of bis-2-MeImH complexes of meso-only-substituted iron(III) porphyrinates [TMP, (2,6-Cl₂)₄TPP, and (2,6-Br₂)₄TPP] have shown that the ΔH^\ddagger values for the porphyrin ring inversion and concomitant ligand rotation range from 46 to $51\ kJ\ mol^{-1}$, while ΔG^\ddagger_{298} ranges from 44 to $50\ kJ\ mol^{-1}$ for $Fe(III)$ complexes and is $67\ kJ\ mol^{-1}$ for the $Co(III)$ complex, $[CoTMP(2-MeImH)_2]^+$.¹² The ΔH^\ddagger values are larger but in the range of those for the bis-4-Me₂NPy and 1-MeIm complexes of $(OETPP)Fe^{III}$, $(F_{20}OETPP)Fe^{III}$, and $(TC_6TPP)Fe^{III}$, whereas the ΔG^\ddagger_{298} values are smaller for $Fe(III)$ but larger for $Co(III)$ than those observed for the $Fe(III)$ complexes of the present study (Table 1). It should be noted that, for the meso-only-substituted iron(III) porphyrinates of the earlier studies,^{12,24-26} the presence of a bulky unsymmetrical axial ligand is required to stabilize the nonplanar (ruffled) ring conformation,⁴⁹ and thus, for the most part, 2-MeImH and 1,2-Me₂Im were used as the axial ligands. The kinetics of ring inversion and ligand rotation of $[OETPPFe(2-MeImH)_2]^+$ could, in principle, have been investigated in this work, given that the dynamics of this complex were clearly observed qualitatively earlier.²⁷ However, it was found that an extremely large excess of 2-MeImH was required to form the bis-ligand complex, even at very low temperatures, and thus, the process of ring inversion could not be isolated from that of ligand exchange.²⁷ The binding constants toward bulky or hindered axial ligands such as 2-MeImH or 1,2-Me₂Im increases in the order $OATPP < TPP < TMP$,⁵⁰ and binding is strongly facilitated by ruffling

(49) Munro, O. Q.; Marques, H. M.; Debrunner, P. G.; Mohanrao, K.; Scheidt, W. R. *J. Am. Chem. Soc.* **1995**, *117*, 935-954.

(50) Nasset, M. J. M.; Shokhirev, N. V.; Enemark, P. D.; Jacobson, S. E.; Walker, F. A. *Inorg. Chem.* **1996**, *35*, 5188-5200.

of the porphyrinate ring, which the octaalkyltetraphenylporphyrinates cannot do as well as can the meso-only-substituted porphyrinates.

The kinetics parameters of ring inversion and ligand rotation in $[\text{TMPCo}(2\text{-MeImH})_2]^+$ and $[\text{TMPCo}(1,2\text{-Me}_2\text{-Im})_2]^+$ differ significantly from those of $[\text{TMPFe}(2\text{-MeImH})_2]^+$: ΔH^\ddagger values are somewhat lower, 48 and 44 vs 51 kJ mol^{-1} ; ΔS^\ddagger values are much more negative (-60 , -62 , and $-84 \text{ J mol}^{-1} \text{ K}^{-1}$), and ΔG^\ddagger_{298} is much larger, 67 and 69 vs 50 kJ mol^{-1} (because of the very negative values of ΔS^\ddagger); this results in a k_{ex}^{298} value almost 1000 times lower for the Co(III) complexes.¹² This difference has been ascribed to the difference in anion [ClO_4^- for Fe(III), BF_4^- for Co(III)],¹² but more detailed studies should be undertaken. Because ΔH^\ddagger is the difference in enthalpy between the ground and excited states, the difference in ΔH^\ddagger observed for $[\text{TMPCo}(2\text{-MeImH})_2]^+$ and $[\text{TMPCo}(1,2\text{-Me}_2\text{Im})_2]^+$ might reflect the case where the ground state is at a somewhat higher enthalpy for the latter, so that smaller changes in enthalpy are required for ring rearrangement. This type of comparative enthalpy profile has been estimated via molecular mechanics (MM2) calculations for $[\text{TMPFe}(\text{Py})_2]^+$, $[\text{TPPFe}(\text{Py})_2]^+$, and $[\text{porphineFe}(\text{Py})_2]^+$.¹⁴ Much less distortion of the porphyrinate core is required for $[\text{TMPCo}(4\text{-Me}_2\text{-NPy})_2]^+$ than for the 2-substituted imidazoles, and we observe a very small ΔG^\ddagger_{298} and very large k_{ex}^{298} .²⁵ Thus, both the ground and excited states of the $[\text{TMPCo}(4\text{-Me}_2\text{NPy})_2]^+$ complex are likely at much lower free energies than the corresponding states of the complexes with 2-substituted imidazoles.

Finally, for the elusive Fe(II) complex, $[\text{TMPFe}^{\text{II}}(1,2\text{-Me}_2\text{-Im})_2]$, which is isoelectronic with the Co(III) complex of the same porphyrinate and axial ligands, the rate constants for porphyrin ring inversion and axial ligand rotation were found to be approximately 1 s^{-1} at both -80 and $-90 \text{ }^\circ\text{C}$.²⁵ Assuming that ΔH^\ddagger for this complex is similar in size to that for the Co(III) or Fe(III) analogue with 2-MeImH ligands, the rate constant for this process at 298 K, k_{ex}^{298} , is $\sim(1-6) \times 10^5 \text{ s}^{-1}$. In the future, we hope that it will be possible to measure the rates of porphyrin ring inversion and axial ligand rotation for the Fe(II) bis-ligand complexes of some of the octaalkyltetraphenyliron(III) porphyrins in which ruffling does not play a major role and the planar axial ligands typically lie close to the $\text{N}_p\text{-Fe-N}_p$ axes rather than the meso carbons.

Conclusions

Both five- and six-coordinate octaalkyltetraphenylporphyrinatoiron(III) complexes provide a unique opportunity to study the kinetics of ring inversion using $^1\text{H NMR}$ 1D

(DNMR) and 2D NOESY/EXSY techniques. The enthalpies of activation, ΔH^\ddagger , range from 24 to 36 kJ mol^{-1} for the complexes of $(\text{TC}_6\text{TPP})\text{Fe}^{\text{III}}$ and from 49 to 63 kJ mol^{-1} for most complexes of $(\text{OETPP})\text{Fe}^{\text{III}}$, with those for $(\text{OMTPP})\text{Fe}^{\text{III}}$ and $(\text{F}_{20}\text{OETPP})\text{Fe}^{\text{III}}$ being between these limits. The entropies of activation, ΔS^\ddagger , vary from $+20$ to $-37 \text{ J mol}^{-1} \text{ K}^{-1}$ for OATPPFe^{III} complexes in CD_2Cl_2 and are slightly more negative for the perfluorinated phenyl analogue, $\text{F}_{20}\text{-OETPPFe}^{\text{III}}$ (ranging from -52 to $-56 \text{ J mol}^{-1} \text{ K}^{-1}$), all of which are relatively small values; ΔS^\ddagger for the $[\text{OETPPFe}(\text{CN})_2]^-$ complex in dimethylformamide (45 and 83 $\text{J mol}^{-1} \text{ K}^{-1}$ over two temperature ranges), where solvation effects differ markedly, cannot be readily compared to the data obtained in CD_2Cl_2 . The only exception to this pattern is $[\text{OETPPFe}(4\text{-CNPy})_2]^+$ in CD_2Cl_2 , which has a very negative ΔS^\ddagger value ($-104 \text{ J mol}^{-1} \text{ K}^{-1}$).⁹ Although we have carefully checked the kinetics data for this system, no errors in the determination of this value are apparent, and in fact, the value was obtained from data determined over a very wide temperature range for which the Eyring plot is linear (see Figure 6).⁹ We have no explanation for the much more negative entropy of activation for that system. The rate constants for ring inversion for all complexes in this study at 298 K are in the range of $10\text{--}10^7 \text{ s}^{-1}$ indicating a large range of porphyrin core flexibilities that increase in the order $\text{OETPP} \approx \text{F}_{20}\text{OETPP} < \text{OMTPP} < \text{TC}_6\text{TPP}$. These flexibilities are related to the amount of porphyrin core distortion and the barrier to axial ligand rotation and can be used as an indirect measurement of the degree of nonplanarity, with the most flexible porphyrin ring (TC_6TPP) being the most planar. Ruffled iron porphyrinates studied previously show k_{ex}^{298} in the range of $1\text{--}10^5 \text{ s}^{-1}$ for $\text{L} = 2\text{-MeImH}$,¹² whereas the corresponding Co(III) complexes have much smaller rate constants ($5\text{--}14 \text{ s}^{-1}$),¹² except for the 4-Me₂NPy complex ($1 \times 10^6 \text{ s}^{-1}$);²⁵ the $[\text{TMPFe}^{\text{II}}(1,2\text{-Me}_2\text{Im})_2]$ complex has $k_{\text{ex}}^{298} \approx (1\text{--}6) \times 10^5 \text{ s}^{-1}$,²⁵ larger than that of the Fe^{III} counterpart by about a factor of 10.

Acknowledgment. We thank the National Institutes of Health, Grant DK-31038 (F.A.W.), for support of this research. Also, we thank Dr. C. J. Medforth for generously providing us with the sample of $(\text{F}_{20}\text{OETPP})\text{FeCl}$. This article was written while F.A.W. was a Visiting Professor and Alexander von Humboldt Senior Awardee in Science at the Physics Institute of the University of Lübeck, and she thanks Professor Alfred X. Trautwein for his hospitality and friendship.

Supporting Information Available: Figures S1–S4 are available free of charge via the Internet at <http://pubs.acs.org>.

IC049090P